

Morphological, chemical, thermal, and mechanical characteristics of Sterculia Foetida (Java-olive) fiber activated carbon for sustainable applications in biodegradable materials

Srinivasa Rao Pedada, R.S.S. Srikanth Vemuri, Ch.V. Kameswara Rao, Srinivas Rao, Golagani Karri Lavanya, Manoj Kumar Regulagadda, Anitha Kumari Mosya



PII: S2211-7156(26)00306-1

DOI: <https://doi.org/10.1016/j.rechem.2026.103332>

Reference: RECHEM 103332

To appear in: *Results in Chemistry*

Received date: 31 January 2026

Accepted date: 18 April 2026

Please cite this article as: S.R. Pedada, R.S.S.S. Vemuri, C.V.K. Rao, et al., Morphological, chemical, thermal, and mechanical characteristics of Sterculia Foetida (Java-olive) fiber activated carbon for sustainable applications in biodegradable materials, *Results in Chemistry* (2024), <https://doi.org/10.1016/j.rechem.2026.103332>

This is a PDF of an article that has undergone enhancements after acceptance, such as the addition of a cover page and metadata, and formatting for readability. This version will undergo additional copyediting, typesetting and review before it is published in its final form. As such, this version is no longer the Accepted Manuscript, but it is not yet the definitive Version of Record; we are providing this early version to give early visibility of the article. Please note that Elsevier's sharing policy for the Published Journal Article applies to this version, see: <https://www.elsevier.com/about/policies-and-standards/sharing#4-published-journal-article>. Please also note that, during the production process, errors may be discovered which could affect the content, and all legal disclaimers that apply to the journal pertain.

Morphological, Chemical, Thermal, and Mechanical Characteristics of Sterculia Foetida (Java-Olive) Fiber Activated Carbon for Sustainable Applications in Biodegradable Materials

Srinivasa Rao^{*a}, Pedada R. S. S. Srikanth, Vemuri^b, Ch.V. Kameswara Rao^c, Srinivas Rao^d, Golagani Karri Lavanya^e, Manoj Kumar^f, Regulagadda, Anitha Kumari Mosya^g.

^aGayatri Vidya Parishad, Engineering College for Women, Visakhapatnam 530 048, India. ^{b&e}Vignans Institute of Engineering for Women, Visakhapatnam 530 049, India ^cLendi Institute of Engineering and Technology Vizianagaram -535005, ^dGitam (Deemed to be University), School of Science, Visakhapatnam 530 045, India. ^{f&g} TDR-Hub Andhra University, Visakhapatnam 530 003, India.

ABSTRACT

In this research paper, activated carbon and biochar were synthesized from *Sterculia foetida* fibers through controlled pyrolysis and chemical activation, using activating agent such as H₃PO₄ under different temperatures and impregnation ratios. The activation process resulted in the development of a hierarchical pore structure consisting of micro- and mesopores, which significantly enhanced the specific surface area and adsorption characteristics of the carbon materials. A comprehensive physicochemical characterization of the prepared materials was performed using X-ray diffraction (XRD), Fourier transform infrared spectroscopy (FTIR), scanning electron microscopy (SEM), energy dispersive spectroscopy (EDS), Differential thermogravimetric analysis (DTG) to evaluate structural, morphological, elemental, and thermal properties. The XRD results confirmed the formation of partially graphitized amorphous carbon structures, while FTIR analysis indicated the presence of oxygen-containing functional groups that enhance adsorption behavior. SEM analysis revealed a highly porous surface morphology formed during carbonization and activation, and EDS confirmed the dominant presence of carbon with minor heteroatoms such as oxygen and nitrogen. The novelty of this work lies in the valorization of *Sterculia foetida* fiber biomass into multifunctional carbon materials, integrating biochar and activated carbon synthesis with advanced characterization to evaluate their structural evolution and adsorption potential. Additionally, the study explores the structure–property relationship between activation conditions and pore development, which is critical for optimizing the performance of biomass-derived carbons. Such materials show promising applications in water purification, pollutant adsorption, energy storage devices, and composite reinforcement materials. Recent research also indicates that carbon materials derived from *Sterculia foetida* can serve as effective electrodes in supercapacitors and as adsorbents for dye removal in wastewater treatment.

Keywords: Cellulosic fiber, Brunauer Emmett and Teller, Thermo gravimetric Method, *Sterculia foetida*, Composite materials

*Corresponding author. E-mail address: raosrp@gmail.com

1.Introduction

Industrial development has been happen more quickly recently, improving availability and efficiency [1,2] However, these advancements have also created severe environmental problems, such as toxic emissions and land, air and water pollution [3]. Research Scientists are progressively exploring natural fibers (NFs) and renewable energy sources as sustainable substitutes for fossil products [4]. NFs have anciently been utilized to make tools and clothes, and they are currently regaining popularity as more environmentally friendly alternatives to artificial materials [5]. NFs have many advantages compared to synthetic fibers, making them more sustainable and eco-friendlier for the industry due to their ecological properties. These include affordability and lightweight, intensify, stiffness and traction strength, heat insulation, temperature stability, resistance to water, non-toxicity, to decay naturally and composability [6,7]. The growing need for sustainable construction, aerospace, and defense materials has spurred research into novel cellulose (CL) fibers. These future generation fibers (NFs) boast desirable properties ideal for reinforcing composites, aligning with the push for environmentally-friendly development [8,9]. NFs' principal components are hemicellulose (HCL), lignin (LG), and wax,



Fig-1: Sterculia-foetida (Java olive) plant fruit

which pose no Adverse effects on humans [10]. The majority of natural fibers come from plants containing CL. Examples include jute, flax, ramie, hemp, and kenaf aloe, pineapple, banana, bamboo, [11]. sisal, and nettles Nature has given abundance resources that are renewable, environmental-friendly having a lot of potential applications for textile fibers and composite materials. Natural fibres can be extracted from various parts of plants and utilized in various applications, from fibre to fabric [12]. Efforts are being made to utilize yearly renewable lignocellulosic fibres for composite applications. Almost one lakh heaps of fibers are consumed yearly [13] over the entire world. have developed Jute fibre reinforced composites that have excellent potential as wood substitutes in view of their low cost, easy availability, saving in energy and pollution free production.[14] have summarized manufacturing methods, characteristics, applications of various nonwovens and composite[15] products from flax fibre. have reviewed manufacturing methods, properties and application of jute nonwoven and nonwoven based composites for various applications. have[16] collected petiole wastes of the *Sterculia-foetida* plant and cut to two different lengths, long and short with average lengths of about 37 mm and 17 mm, and used for preparation of eco-friendly lightweight pervious concrete.

This approach can reduce environmental pollution while also providing low density and adequate strength to pervious concrete .Benefits of natural fibers over artificial fibers adopt low cost, less density, reprocessed and biodegradability along with their carbon dioxide neutral life cycle [17] *Sterculia- foetida* plants are commonly known as bastard poon tree, java olive tree, wild almond tree, and skunk tree. Green *Sterculia foetida* fruit shell fiber has been extracted and used in the present research work, employing the opinion to utilize such waste fruit[18] *Sterculia foetida* is a tropical tree, while nature has given plenty of renewable and environment-friendly resources. It was found in the literature that *Sterculia foetida* fruit shell extract can impart natural coloration along with inherent functional finishes such as antibacterial and ultraviolet protection properties on cotton [19], silk [20]), wool [21], and linen fabric (Man-made fibers are stronger, more durable, cheaper and less delicate to temperature and moisture than natural fibers [22] Natural fibers in simple definition are fibers that are not synthetic or manmade. They can be sourced from plants or animals [23]. The utilization of natural fiber from both resources, renewable and nonrenewable such as oil palm, sisal, flax, and jute to produce composite materials, gained important attention in the over the last few years so far. One of the major challenges associated with natural fibers is their hydrophilic nature, which

results from the presence of hydroxyl groups [24].in cellulose and hemicellulose. This characteristic leads to poor compatibility with hydrophobic polymer matrices such as polyester, polypropylene, and epoxy.to overcome this limitation, several surface modification techniques have been investigated. Alkali treatment (NaOH treatment) is one of the most commonly used methods for improving [25,26] fiber–matrix adhesion. This treatment removes impurities such as lignin, wax, and hemicellulose from the fiber surface, thereby increasing surface roughness and improving interfacial bonding Other chemical treatments such as silane treatment, acetylation, and peroxide treatment [27], have also been explored to enhance fiber performance. These treatments reduce moisture absorption and improve dimensional stability of natural fiber composites.

2.Experimental methods

Materials and methods

2.1 Extraction of *Sterculia- foetida* fruit shell fiber

The *Sterculia- foetida* materials were collected from Andhra university Botany department garden at Visakhapatnam, India. The fibers were extracted from the bark (bast fiber) and sometimes from fruit/seed structures red fruit shell of the *Sterculia foetida* plant, as shown in (Figure 2), *Sterculia foetida* (Wild Almond / Java Olive) is a lignocellulosic biomass source. Fibers are mainly obtained from the carefully remove outer bark strips without damaging the tree. Collect bark in clean containers. Wash with distilled water to remove soil and debris. To obtain fiber-rich bast layer from the bark Method: Water Retting cut bark into small strips (10–25cm).Immerse in clean water (ratio 1:25 biomass to water).keep submerged for 7–15 days at room temperature .Microbial activity breaks down pectin and hemicellulose.. Treat with 3–5% NaOH solution at 50–80 °C for 1–3 hours. Wash thoroughly until neutral after retting, remove bark from water. Gently beat or scrape the bark. Separate long fibers manually. Wash again to remove decomposed matter Light brown color Lignocellulosic composition Suitable for: activated carbon production, Composite reinforcement, Textile and rope applications and Bio-adsorbent preparation.

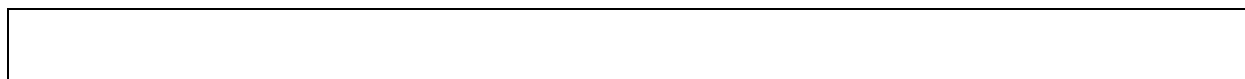




Fig-2: Sterculia- foetida Fiber Extraction Process

2.2 Preparation of *Sterculia foetida* fruit shell fiber composite

Extracted *Sterculia foetida* fruit shell fibers was utilized to prepare epoxy resin-based composites. Both the fibers were cut into 150 mm length. Epoxy resin and the corresponding hardener was supplied by Sigma- Aldrich India For the preparation of composite, a stainless steel mould was used. The mould cavity was coated with a thin layer of silicone oil solution, which acts as a releasing agent. Epoxy resin and fibers are mixed with 20:5 ratios and benzyl alcohol were added as diluents and the mixture was mixed thoroughly by a mechanical stirrer for 25 min. The composites were prepared by hand lay-up technique with fiber loading of 65% for both the cases and subjected to post-curing in a the compression molding machine at 150 °C for 1 h at 125 psi pressure

2.3 Water absorbency analysis of the composite material

This testing was done according to ASTM D570 standard method. Samples were cut 5” × 2” according to standard and dried at 75 °C in an oven for 48 h followed by cooling in a desiccator for 10 min and immediately weighed, then immersed in water for 24 h, wiped with a cloth and weighed. The difference between initial weight and final weight was noted and the water absorbency percentage was calculated as per given equation.

$$\text{Water absorbency (\%)} = \frac{(W_i - W_f) \times 100}{W_i}$$

Where, W_i = The initial weight of the sample and W_f = The final weight of the sample

Chemical composition and physical properties of *Sterculia- foetida* fruit shell fiber.

Constitution	Composition (%)
β-Cellulose	46.44
Hemicellulose	27.27
Lignin	14.28.
Ash	3.9
Extractive	14.28 ± 0.2
Density	0.495-0.6 g/cm ³
Moisture content	7.2–7.5
Moisture regain	4.9-3.4
Tensile strength	542.17 gf
Elongation	4.11%

Table -1: Analysis of water absorbency at *Sterculia-foetida*

3. Results and discussion

Determination of chemical composition and physical properties of *Sterculia-foetida* fruit shell fiber. The chemical composition of *Sterculia-foetida* fruit shell fiber was obtained by a mechanical extraction method is reported in (Table-1). The raw fibres are composed of cellulose, hemicelluloses, lignin, ash and extractives. In other words, these fibers are basically cellulose-dominated. However, they have significant lignin content like other lignocellulosic fibers, most closely to nearly 14% lignin [28] (Pandit et al., 2018b). Tensile strength, moisture content and moisture regain of the *sterculia-foetida* fruit shell fiber was found to be 542.17 gf with an elongation at break at 4.11%, moisture content 7.2–7.5 % and moisture regain 4.9–3.4 %

3.1 Differential Thermogravimetric (DTG) of *sterculia-foetida* fiber shell particulates

Thermal analysis is the concept that purely reflects the decomposition reactions that occur at the molecular level of the materials [29] with variation in temperature. For the analysis, around 20–30 milligrams of sample were taken in an Al_2O_3 crucible at heating rate $10\text{ }^\circ\text{Cmin}^{-1}$, from room temperature 27 ° to $600\text{ }^\circ\text{C}$ in the presence [30] of nitrogen at flow rate of 30ml/min. Thermogravimetric weight loss curve was plotted against temperature. The apparatus provides for the continuous measurement of sample weight as a function [31] of temperature (DTG) (Fig. 2 & 3) shows the DTG curve of raw, carbonized and activated carbon of both *sterculia-foetida* shell. From figures it is clear that initial decrease in weight loss completed below $150\text{ }^\circ\text{C}$ is due to the moisture loss from the all the material at this temperature. Next step is the thermal degradation of biomass. In thermal degradation, firstly at 155 ° – $169\text{ }^\circ\text{C}$ lignin is the first component which decomposes followed by decomposition of hemicellulose [32] which starts from 250 ° – $350\text{ }^\circ\text{C}$. After, hemicelluloses decomposition in the final step major weight loss occurred within the temperature range of 375 ° – $450\text{ }^\circ\text{C}$ as a consequence of the cellulose decomposition. The same types of thermal behavior were reported by Nunn et al. [33]. They reported that the decomposition of cellulose and lignin took place at a wide temperature range of 250 ° – $350\text{ }^\circ\text{C}$ and 200 ° – $400\text{ }^\circ\text{C}$, respectively. Furthermore, the rate of decomposition was slow. Zeriouh et al. [34] reported that the decomposition of hemicellulose, cellulose and lignin occurred at temperature [35] ranges of 200 ° – 300 ° , 250 ° – 350 ° , and 350 ° – $450\text{ }^\circ\text{C}$, respectively.

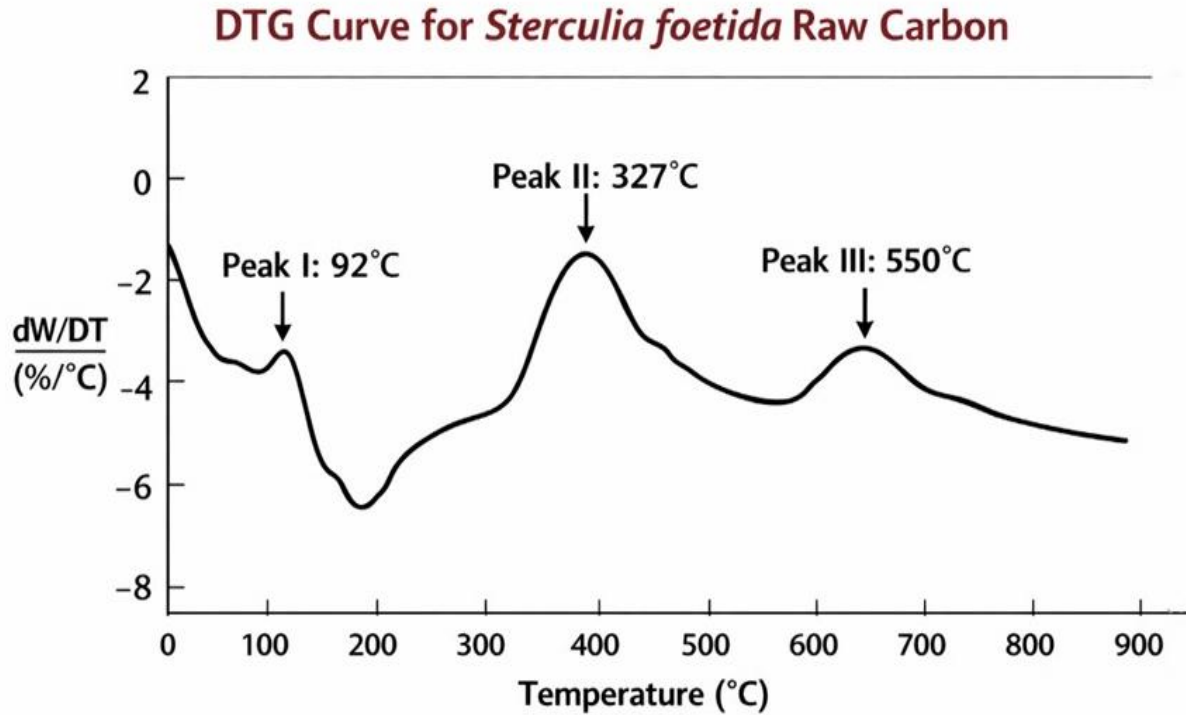


Fig. 3: DTG of *Sterculia-foetida* raw carbon black shell particulates

Researchers already reported that lignin is the first component which decomposes at low temperature (160-170 °C). For the carbonized material the stages are varied when compared to raw particles the degradation temperature (36) also increases this is due to conversion of lignin into carbon material. The stages are reduced at the higher carbonization temperature. Due to activation the carbon content are increases hence the carbon has higher thermal resistance this is confirmed by the DTG of activated carbon line Main DTG Peak \approx 320–330 °C Represents maximum rate of mass loss. Caused by decomposition of residual hemicellulose and cellulose fragments remaining after activation. Indicates thermal degradation (37) of unstable oxygen-containing functional groups. 200–280 °C Region, Gradual weight-loss rate. Associated with dehydration and removal of volatile organic compounds. 330–400 °C Region, DTG curve becomes smoother. Indicates formation of a stable carbon matrix and beginning of aromatic carbon structure development.

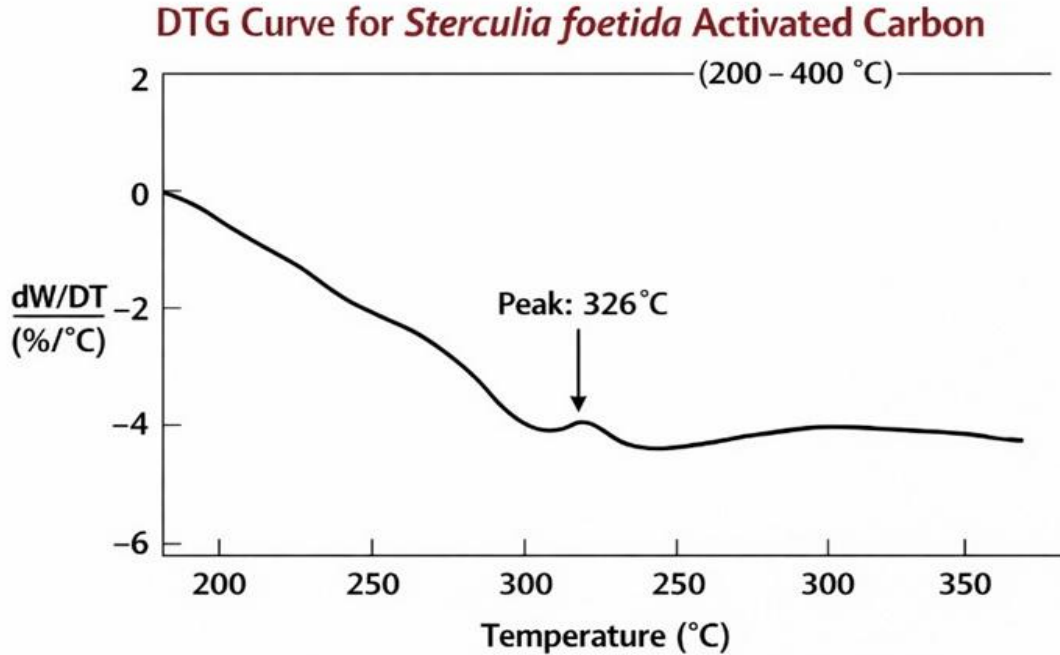


Fig 4: DTG of *Sterculia foetida* activated carbon shell particulates

3.2 Effect of Filler Content on Tensile properties of *Sterculia-foetida* fiber shell particulate composite

Effect of various filler content such as raw carbon black and activated carbon black particles prepared from *sterculia-foetida* shell on tensile strength of the composites is depicted in Fig (5A). It is observed from the plot that the tensile strength (38) of the composites found to increase with increase in the filler content. However, with filler content of 15wt% (raw) the tensile strength found to be 4.367×10^8 Dyne/Cm² compared to neat epoxy strength of 21.43MPa. Thereafter with higher filler content it decreases. The tensile strength of the composites filled with carbon black prepared from *sterculia-foetida* shell particles at three carbonization temperature (400°C - 800°C) were also carried out. It is found that carbon black particle enhances the strength of the neat polymer composite. *Sterculia-foetida* shell carbon black composite reinforced with carbon

Composite samples	Filler (wt%)	Tensile Strength (MPa)	Flexural Strength (MPa)	Tensile Modulus (GPa)	Flexural Modulus (GPa)	Hardness (Hv)
Epoxy	0	21.43	43.59	0.68	0.79	20.42

Raw	5	28.62	55.27	0.87	1.43	24.52
	10	35.63	69.09	1.46	2.315	23.36
	15	43.67	75.17	1.70	2.70	28.54
	20	39.85	67.19	1.64	2.52	24.66
400°C CB	5	36.77	64.05	1.71	1.49	24.32
	10	45.67	74.77	1.69	2.60	26.59
	15	52.38	93.07	2.58	2.84	26.59
	20	45.59	82.34	2.42	2.74	23.37
600°C CB	5	32.80	73.57	1.97	2.80	23.27
	10	50.25	59.54	2.65	2.69	25.19
	15	63.49	80.45	2.78	2.52	24.97
	20	52.75	83.49	2.69	2.51	25.38
800°C CB	5	44.43	73.29	1.89	2.38	23.87
	10	59.61	79.52	2.56	2.61	24.52
	15	57.29	82.56	2.60	475	26.29
	20	57.50	83.45	2.48	2.39	25.58
ACB (800°C)	5	55.39	92.75	2.43	2.49	27.96
	10	66.54	871.54	2.48	2.76	25.27
	15	59.87	86.98	2.69	2.98	30.91
	20	52.57	79.72	2.73	2.74	32.43

Table 2: Mechanical properties of Sterculia-foetida activated carbon particulate composite

black particulate prepared at 800°C with 10 wt% filler gives optimum strength of 59.61MPa as recorded from the experiment shown in Table 2, Addition of activated carbon black particulates with neat epoxy shows highest tensile strength compared to other non-activated filler composites. 10wt% activated carbon black composite gives superior strength as compared to other non-activated composite. This is more strength compared to strength of neat epoxy. This might have happened removal of volatile substances, formation of porous structures and increase in carbon content which forms some ceramic carbide (Silicon carbide, Zinc carbide) at the time of carbonization process followed by activation Formation of these hard-ceramic particles increases the strength of the resulted composites. Beyond 10wt% of filler content decrease in strength might

be due to poor filler matrix interaction Fig.(5 B&C). shows the plot of tensile modulus of sterculie-foetide activated carbon and raw carbon black shell particulate composites. It is clearly observed that the tensile modulus of the raw, carbon black and activated carbon black of sterculie-foetide

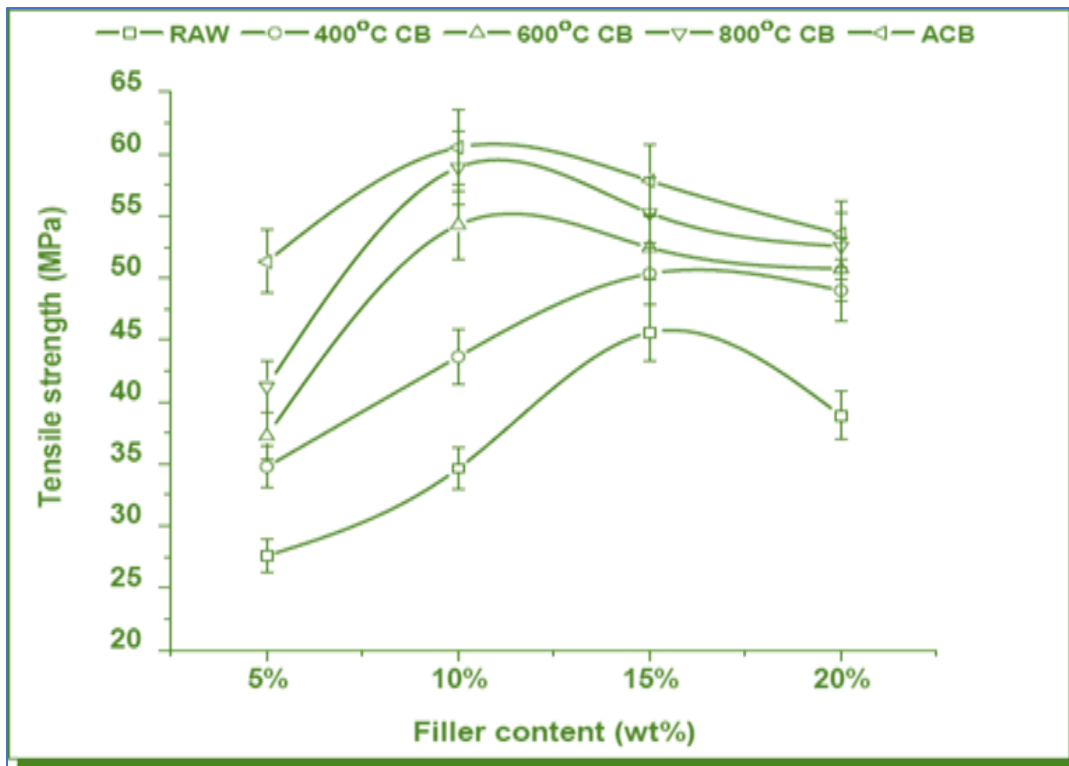


Fig. 5(A): Filler Content on Tensile properties of Sterculia-foetida activated carbon 400 °C particulate composite

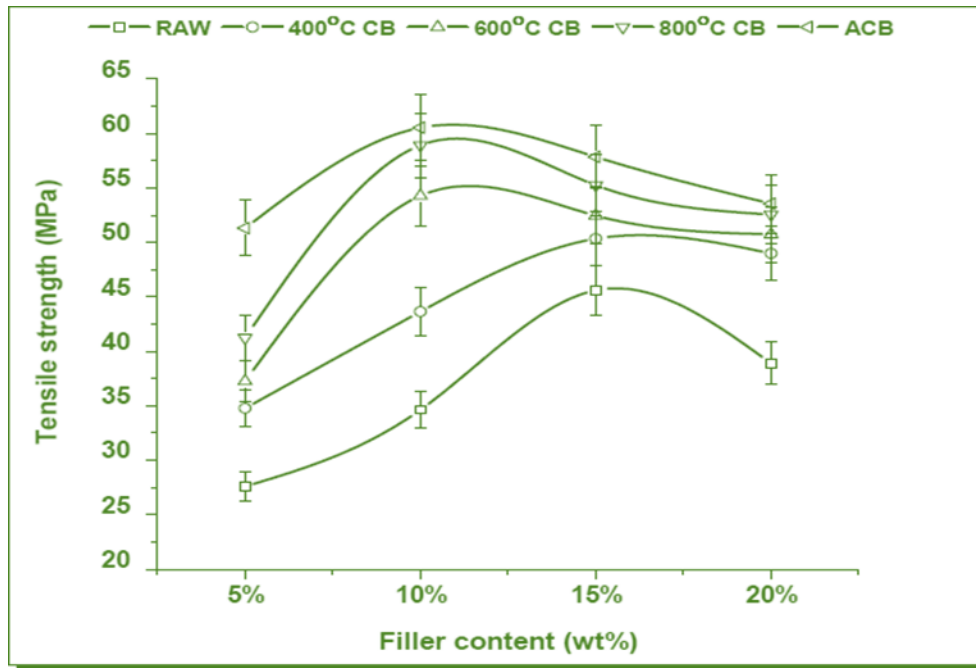


Fig. 5(B): Filler Content on Tensile properties of Sterculia-foetida activated carbon 600 °C particulate composite



Fig. 5(C): Filler Content on Tensile properties of Sterculia-foetida raw carbon particulate composite

shell filled epoxy composite follow the similar trend as observed in the tensile strength. Among all the composites, the highest Tensile modulus of 2.78GPa is observed for composites filled with 15wt% at 600 °C activated carbon black particulates. The modulus of the material increases as the carbonization temperature increases and it is found to be maximum for activated carbon

4. Morphological Characteristics

4.1 Scanning Electron Microscopy (SEM)

Scanning Electron Microscopy (SEM) technique (SEM can perform three-dimensional measurements at the micro-nano scale. This is possible because SEM micrographs have a large depth of field due to their narrow electron beam. This gives the micrographs a *property* of three-dimensional *aspect* that can be used to understand the surface structure of a sample. SEM can provide a wide range of magnifications, from about 12 times to over 500,000 times) was employed to investigate the surface physical morphology of sterculie –foetide fiber shell derived carbon black and activated carbon black. Fig.6(A-C) shows the SEM micrographs of the raw carbon black and activated carbon prepared from sterculie –foetide shell particles under different conditions. SEM technique was employed to observe the surface physical morphology of sterculiea-foetide fiber shell derived carbon black and activated [39] carbon black. It also gives information about the changes induced by carbonization and activation of raw Fig.6(A) sterculie-foetide fiber shell particles. It also can be seen from Fig.6(A) that the surface of the raw sterculiea-foetide was dense and planar and also no porous found on the surface [40]

At higher magnification micron particles are clearly observed on the surface. For the carbon black pyrolyzed at 400°C of activated carbon sterculie-foetide fiber shell particles with a retention time 1h, the micrograph showed some porous on the surface is shows in Fig.6(B). Initially some porous structure is developed because of removal of volatile mater from the raw particles. Also at 13000x magnifications there are small porous [41] structure has clearly observed in the surface of 400°C carbon black particles is shown in Fig. 6(C), as the carbonization temperature increases from 600-800°C, the diameter of the carbon black particles are smaller is shown in Fig. 6(C).Also the micros porous are gradually increasing in the surface of 600°C carbon black particles. Considerably the area of the developed porous structure

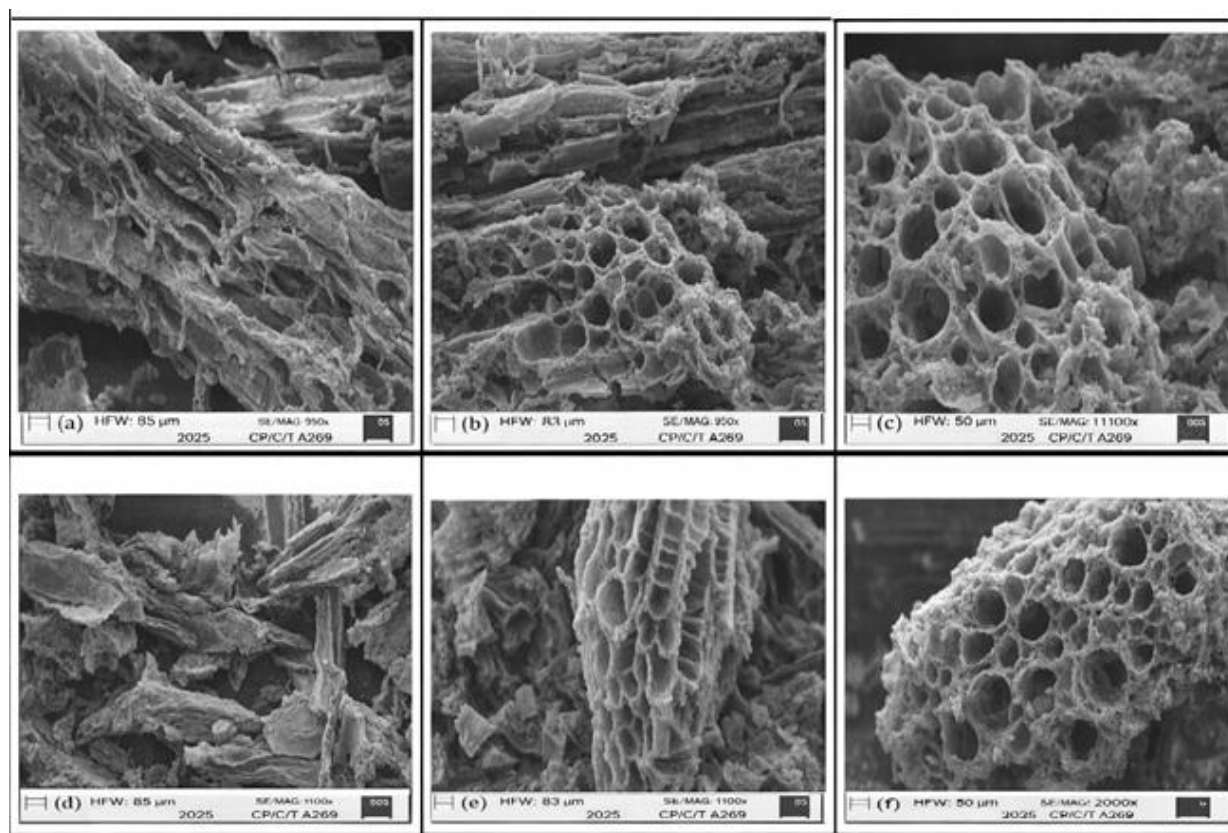


Fig6(A): SEM- images of Sterculia-foetida raw carbon black composites

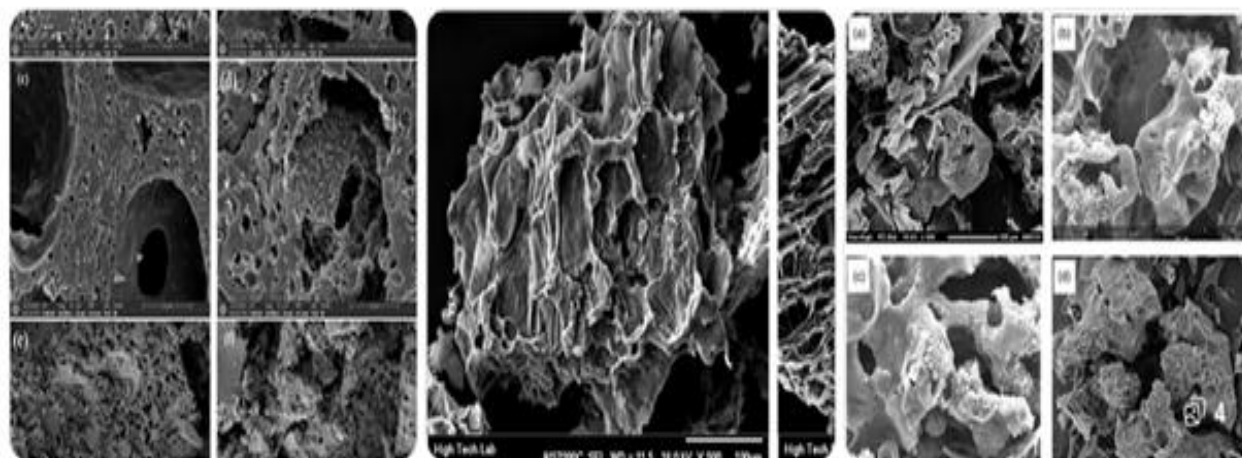


Fig.6(B): SEM images of Sterculia-foetida activated carbon black composites at 400°C

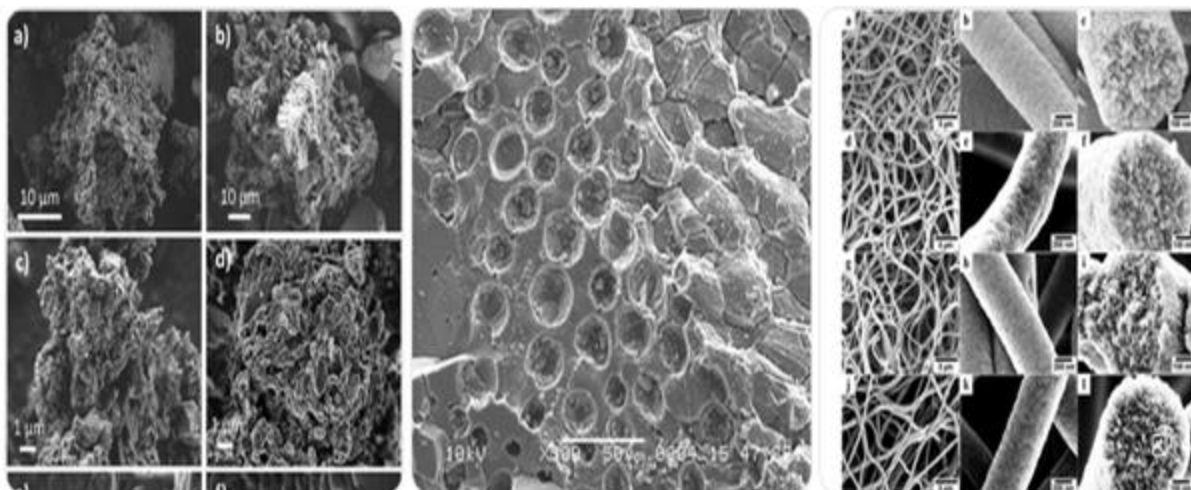


Fig.6(C): SEM images of Sterculia-foetida activated carbon black composites at 600-800 °C

has been increased is shown in Fig. 6(C). The micrograph of the carbon black at 800°C for 1h shows that there were many pores over the surface, forming a system of advanced pore structures. Due to this well-developed pore [42] the carbon black possessed high BET surface area and adsorptive capacity. It is because of the reduction of more volatile matter during 800°C carbonization lead to the development of pores on the surface of the carbon black particles. At this temperature the area of the porous structure has also been increased which is proven by the BET analysis. One interesting thing is that within the porous structure some particles are found in nano range at 50000x higher magnifications. After every stage of carbonization, the area of the porous structure in the surface are wider than the size of the existing pores.

After activation of sterculie-foetide fiber shell a particle, the external surface is chemically activated by phosphoric acid (H_3PO_4) is rich with cavities. There are numerous micropores with regular size are developed in the surface which is clearly observed from the Fig.6(C), as well as the area of the pores are significantly increases as compared to other carbon and non-carbon particles. The clearly porous structure of the H_3PO_4 activated carbon resulted from the dissipation of during carbonization, leaving the empty space previously occupied by the phosphoric acid. Due to the effect of activation at 800°C.

4.2 Energy Dispersive Spectroscopy (EDS)

The microstructure of the Sterculia-foetida fiber shell particle reveals that the size and shape of the particles vary however, they can be sorted into three main groups –

prismatic, spherical and fibrous. The prismatic particles consist mainly of Si and O. The spherical ones contain Si, Na and O as well as Ca and Al. The fibrous ones consist of only C [43]. Fig. 7(A-C), show the inspection spectra of sterculia-foetida fiber shell particulate surface elements acquired for sterculia-foetida. The surface of raw particulates exhibits spectra containing mainly carbon, oxygen, silica, aluminum with small amount of zirconia and calcium is shown in Fig. 7(A). Due to pyrolytic decomposition non-carbon elements are slowly removed from raw sterculia-foetida fiber shell particulates at various carbonization temperatures i.e.400°C- 600°C & 800°C. Hence the carbon, silicon and zirconia percentage within the raw particulates is gradually increasing which is clearly observed from the Fig. 7(A), 7(B) and 7(C).Also from the Fig.7(C). it can be noticed that after chemical activation of raw fiber shell particulate at 800°C carbonization temperature the carbon and silicon percentage drastically increase as compared to non-activated carbon particles.

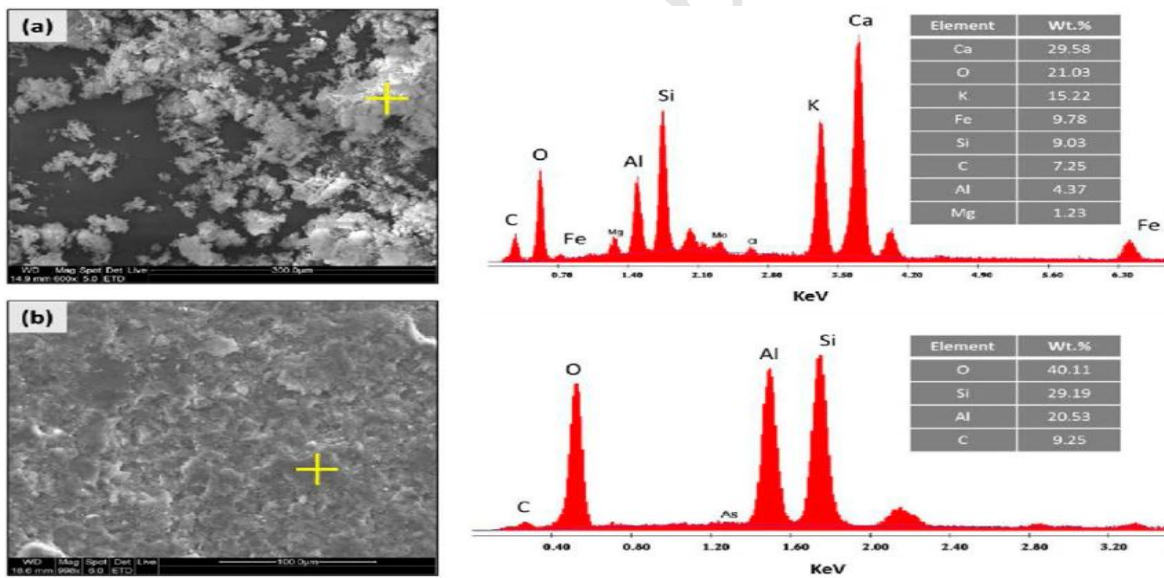


Fig. 7(A): EDS of carbonized *Sterculia foetida* raw carbon back fiber shell composite

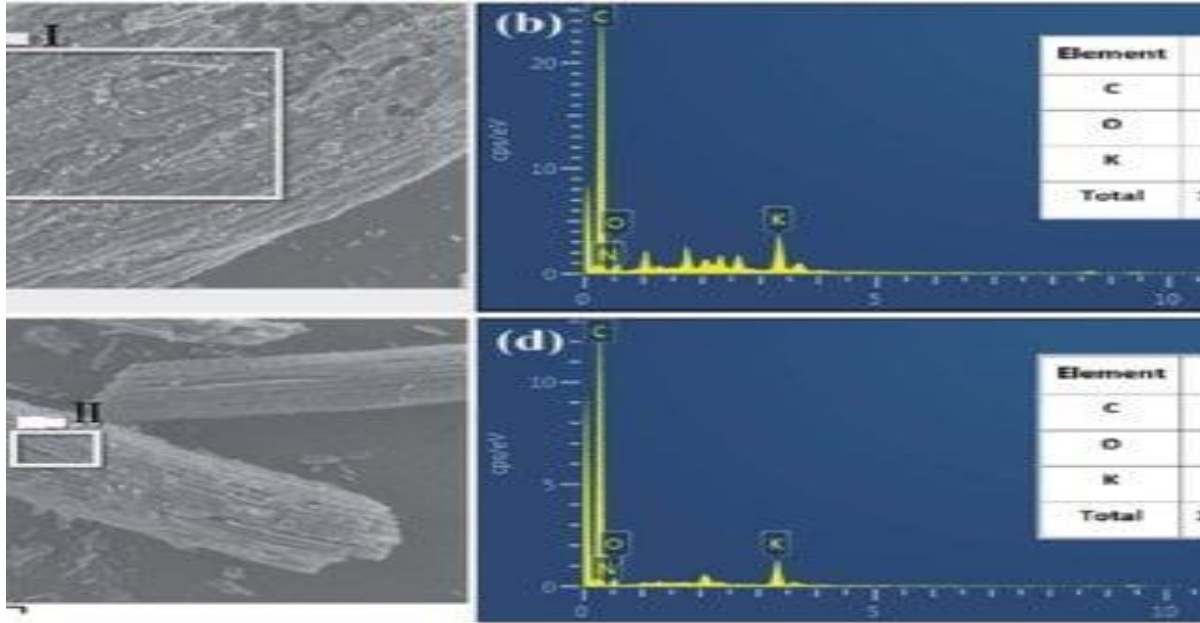


Fig.- 7(B): EDS of 600°C *Sterculia foetida* activated carbon black fiber shell composite

Here, also similar observations are found that carbon content increases at every stage of carbonization process which is shown in Figures 7(B), & 7(C). Also the carbon and silicon percentage is more as compared to other non-activated particles. Finally activated carbon black particles of *sterculie-foetide* contains some hard ceramic particles like SiO_2 , Al_2O_3 and zirconia. Hence these particulate can be used as reinforcement in various polymer matrixes

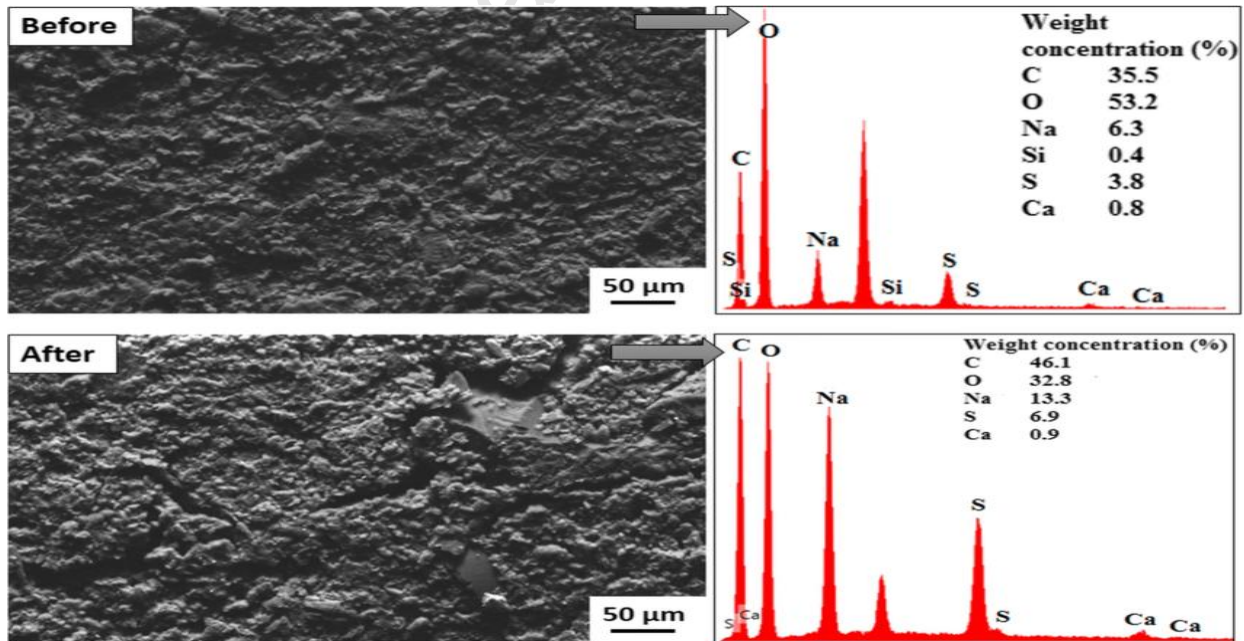


Fig. 7(C): EDS of 800°C *Sterculia foetida* activated carbon black fiber shell composite

4.3 Crystal Structure Transition

Raw carbon (unactivated biomass) derived from *Sterculia foetida* shell typically exhibits an amorphous carbon structure with partial graphitic characteristics. X-ray Diffraction (XRD) analysis is used to determine the crystallinity, phase composition, and structural order of the carbonized material. *Sterculia foetida* fiber from is a lignocellulosic material, primarily composed of cellulose, hemicellulose, and lignin. XRD analysis typically reveals a semi-crystalline cellulose Figure 8(A), embedded within an amorphous matrix. The XRD patterns of raw carbon black and activated carbon black *sterculia-foetida* shell particles have been presented in Figures 8(A-B), It is clearly observed from the figures that XRD signals of [44-47] powder sample contains large amount of noises in it. This behavior confirms the amorphous structure of carbon. As is evident from these figures the sharpness of the peaks of carbon black particles increases as the carbonization temperature increases (400-800°C). Correspondingly, after activation of raw particles with phosphoric acid the sharpness of the peak drastically increases as compared to non-activated particles is shown in Figures 8(B).

It is observed from Figure 8(A), that the raw *sterculie-foetida* shell particles at 2θ scale gave peaks at 13.428, 21.760, 35.709, 45.467 and 46.934. Out of these 13.428, 21.760, 35.709 are mainly of the crystalline cellulose and the remaining amorphous areas are due to lignin and hemicelluloses component in shell particles. Phases of these peaks as: Mg_2SiC , SiO_2 , Al_2O_3 , MgO , this revealed that this particle has some of the composition of hemicelluloses, cellulose and lignin that has been confirmed by the literature [48]. The XRD patterns of all the *sterculie-foetida* shell particles presents broad profiles (containing only 110,110, 200, and 004 bands) centered in angular position near to graphite, which indicates hard carbon. This indicates the strong peak at $\sim 22^\circ$ confirms crystalline cellulose. The broad background hump (18–21°) indicates amorphous lignin and hemicellulose. Typical crystallinity index (CI): 35–55% (raw fiber). The X-ray diffraction (XRD) analysis of raw carbon derived from *Sterculia foetida* shell (unactivated biomass) typically exhibits a broad and low-intensity diffraction peak around $2\theta \approx 22\text{--}26^\circ$, which corresponds to the

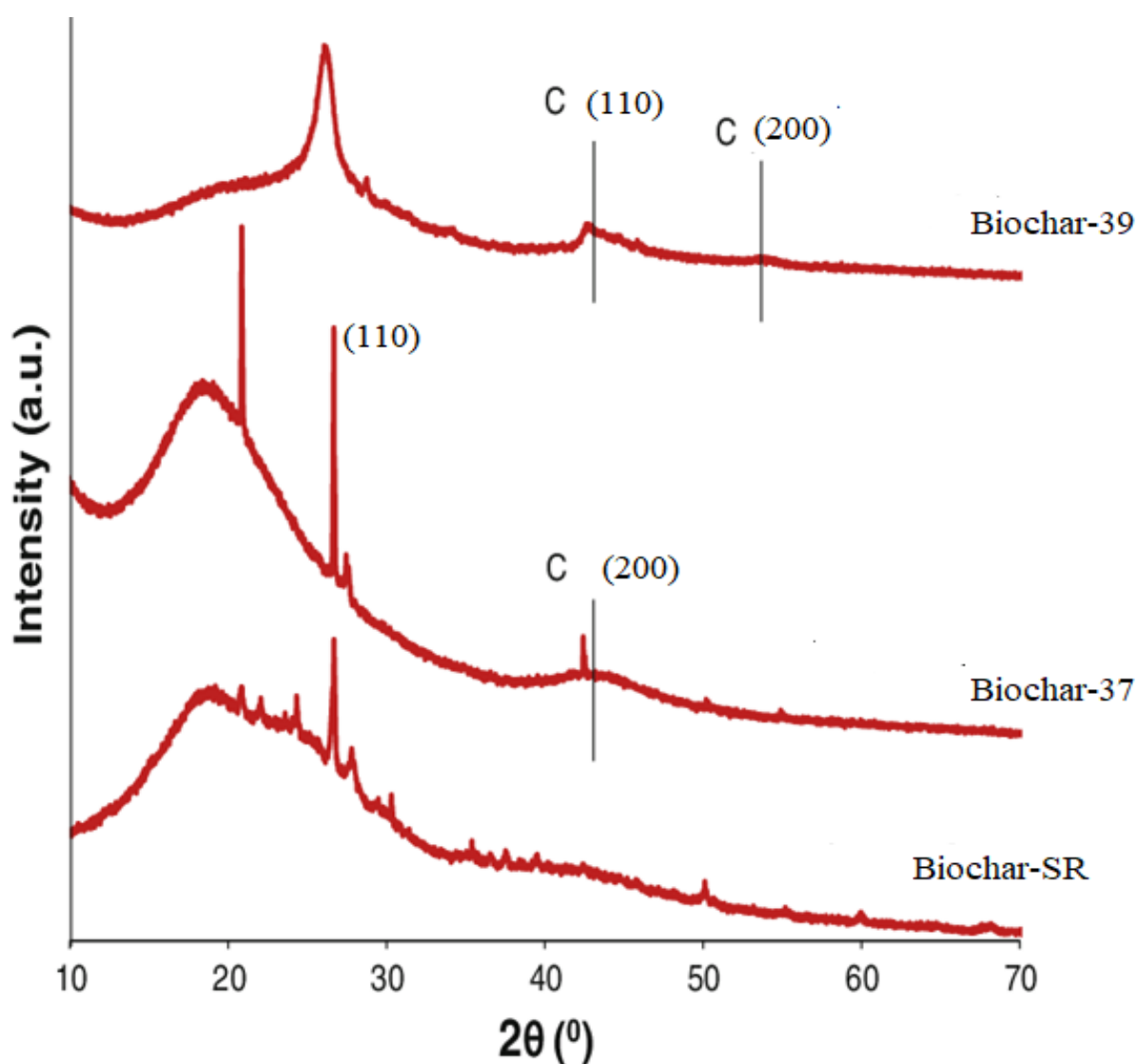


Fig.-8 (A): XRD Analysis of *Sterculia foetida* Shell – Raw Carbon (Unactivated Biomass)

(002) plane of amorphous carbon. This broad peak indicates that the carbon structure is largely disordered and non-graphitic, which is characteristic of lignocellulosic biomass materials before chemical or physical activation. The absence of sharp crystalline peaks suggests that the raw carbon contains predominantly amorphous carbon matrices formed from the decomposition (49) of cellulose, hemicellulose, and lignin components during the initial carbonization process. In addition, a weak and broad peak near $2\theta \approx 42\text{--}45^\circ$ may appear, corresponding to the (100) plane of turbostratic carbon, indicating the presence of

small and poorly organized aromatic carbon layers. These diffraction patterns confirm that the carbon produced from *Sterculia foetida* shell in its unactivated state possesses low crystallinity and a highly disordered microstructure, which is favorable for further activation processes aimed at developing microporous structures and increasing surface area for applications such as adsorption, filtration, and energy storage materials

2 θ (°)	Plane (Cellulose)	Structural Assignment
14–16°	($\bar{1}10$)	Crystalline cellulose
16–18°	(110)	Cellulose
22–23°	(200)	Main crystalline peak
34–35°	(004)	Higher order reflection
18–21°	—	Amorphous lignin/hemicellulose

Table-3: Typical XRD Characteristic Diffraction Peaks of raw *Sterculia- foetida*

Typical XRD Pattern of H₃PO₄-Activated Carbon

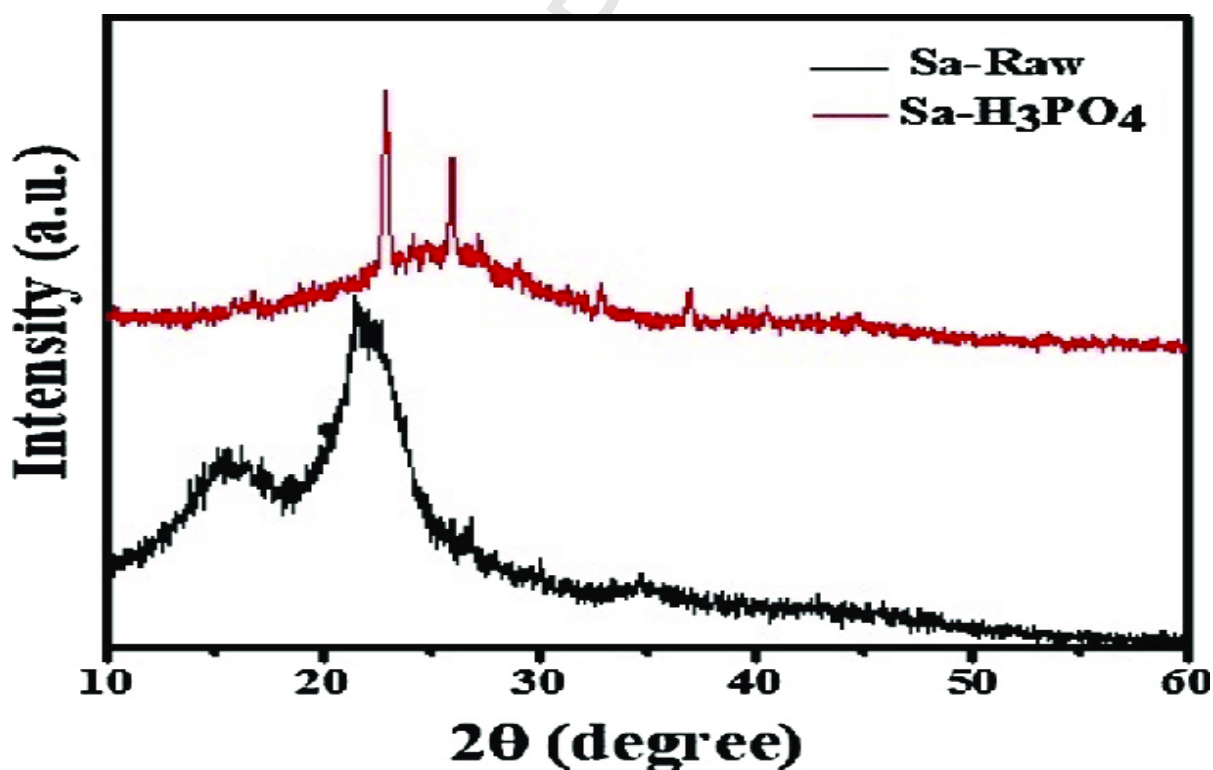


Fig-8 (B): XRD Analysis of *Sterculia foetida* Shell – Activated Carbon

The XRD analysis of activated carbon produced from *Sterculia foetida* shell in the presence of phosphoric acid (H_3PO_4) typically reveals a broad diffraction peak around $2\theta \approx 23-26^\circ$, corresponding to the (002) plane of amorphous carbon. Compared with raw carbon, the peak becomes slightly broader and less intense, indicating that the activation process with H_3PO_4 promotes the development of a highly disordered and porous carbon structure. Phosphoric acid acts as a dehydrating and cross-linking agent, which enhances the breakdown of lignocellulosic components such as cellulose, hemicellulose, and lignin during thermal treatment.

This process leads to the formation of aromatic carbon sheets arranged in a turbostratic manner, resulting in predominantly amorphous carbon with low crystallinity. A weak and broad peak may also appear around $2\theta \approx 42-44^\circ$, corresponding to the (100) plane, which indicates the presence of short-range ordered graphitic microdomains within the carbon matrix. The absence of sharp crystalline (50) peaks confirms that the H_3PO_4 -activated carbon possesses a highly disordered structure with expanded interlayer spacing, which is beneficial for the development of micropores and mesopores. Such structural characteristics contribute to higher surface area, improved pore volume, and enhanced adsorption capacity, making the activated carbon suitable for applications in water purification, gas adsorption, catalysis, and electrochemical energy storage systems.

Characteristic Diffraction Peaks

2θ ($^\circ$)	Plane	Structural Assignment	Observation
22–26 $^\circ$	(002)	Graphitic layer stacking	Broad peak
42–45 $^\circ$	(100) / (101)	In-plane aromatic ordering	Weak broad peak
15–20 $^\circ$	—	Residual amorphous carbon	Diffuse hump
>50 $^\circ$	—	Minor mineral residues (if any)	Very weak peaks
2θ ($^\circ$)	Plane	Structural Assignment	Observation

Table-4: Typical XRD Characteristic Diffraction Peaks of Activated carbon in *Sterculia- foetida*

Temperature	d002 (nm)	Crystallinity	Structural Order
200 $^\circ$ C	~0.38–0.40	Very low	Highly amorphous
400 $^\circ$ C	~0.36–0.38	Low	Developing carbon layers
600 $^\circ$ C	~0.34–0.36	Moderate	Turbostratic
800 $^\circ$ C	~0.34	Higher (but broad peaks)	Partial graphitic domains
Temperature	d002 (nm)	Crystallinity	Structural Order

Table-5: Typical XRD Structural Interpretation of Activated carbon in Sterculia- foetida

that the Sterculie-foetida carbon black particles contain microcrystalline particles of the order of graphite like planes arranged turbo statically as suggested by Emmerich et al. [51]. The change in (002) and (100) diffraction profiles for carbon black and activated carbon black of sterculie-foetida fiber shell particles, prepared at various temperature 400°-800°C with increase in carbonization temperature is shown in Figures 8(B) The relative structural ordering in these carbon black, in relation to their carbonization temperature, was evaluated not only by the most advantageous lattice parameters [52] these broad profiles sharpened and some annular shifting of the lines in the direction of graphite characteristic values with increase of carbonization temperature.

This result indicates that carbon atoms of carbonized sterculie-foetida fiber shell particles are rearranged from disorderly to orderly and the crystalline structure [53,54] improves remarkably with increasing carbonization temperature as well as reducing the amorphous cavity of the particles. Also SiO₂, Al₂O₃, MgO small peaks are present in carbon black particles. After activation of raw sterculie-foetida shell particles with H₃PO₄ chemical activating agent at 800°C activation temperature, these two broad peaks $2\theta=22^\circ$ and 43° which corresponds to the peak of graphite [55] is shown in Figure 8(B). It can be clearly observed from the figure that after activation the two peaks are broad and carbon and silicon dioxide is present in that phase. Similar observations are also found by Kumar et al. [56] in their research work. From the result it is concluded that at every carbonization temperature the two peaks are gradually sharpened and move towards the crystallinity.

The activated carbon samples with broad peaks and absence of sharp peak that revealed predominantly amorphous structure, which is an advantageous property for well-defined porous adsorbents [57]. Broad peaks found at around 22° - 24° for all the samples confirm that the samples are non-graphitized and can have high micro porous structure [58]. Also, it corresponds to the presence of silica and carbon there by confirming the existence of amorphous SiO₂ in carbon particles. also the peak intensity of carbon and activated carbon black particulates is gradually increases. The broad peak at $2\theta = 24^\circ$ corresponds to the presence of silica and thereby confirming the existence of amorphous SiO₂ in activated charcoal. In the entire cases relative intensity and diffraction peaks of carbon and activated carbon black samples were increased gradually as the carbonization temperature increases. As the carbonization temperature

increases is shown in Figures 8(B). The intensity of diffraction peak also increases due to removal of impurities. As the carbonization temperature increases two broad peaks (002) and (97) are observed and slowly sharpen move towards the graphite region. Activated carbon black particles are showing broad and sharp peak than other non-activated particles. Some peaks are indicating to SiO₂ and other small peak indicates to carbon element

Functional group analysis using FTIR-Spectra

4.4 FTIR analysis of Sterculia-foetida fiber shell particulates

The Fourier transform spectra of the sterculia-foetida fruit shell fiber is shown in (Fig. 9-A,B), a broad band in the region of 3390 to 3400 cm⁻¹ that can be consider to the O–H stretching vibration of cellulose molecules. Possible assignment of frequencies of functional group (Table-6-7), in raw carbon sterculia foetida fibre was found at 3400—3300 cm⁻¹(Raw-carbon) as O–H stretching of α -cellulose, 2930 cm⁻¹ as C–H [59] stretching, 2256 cm⁻¹(Activated

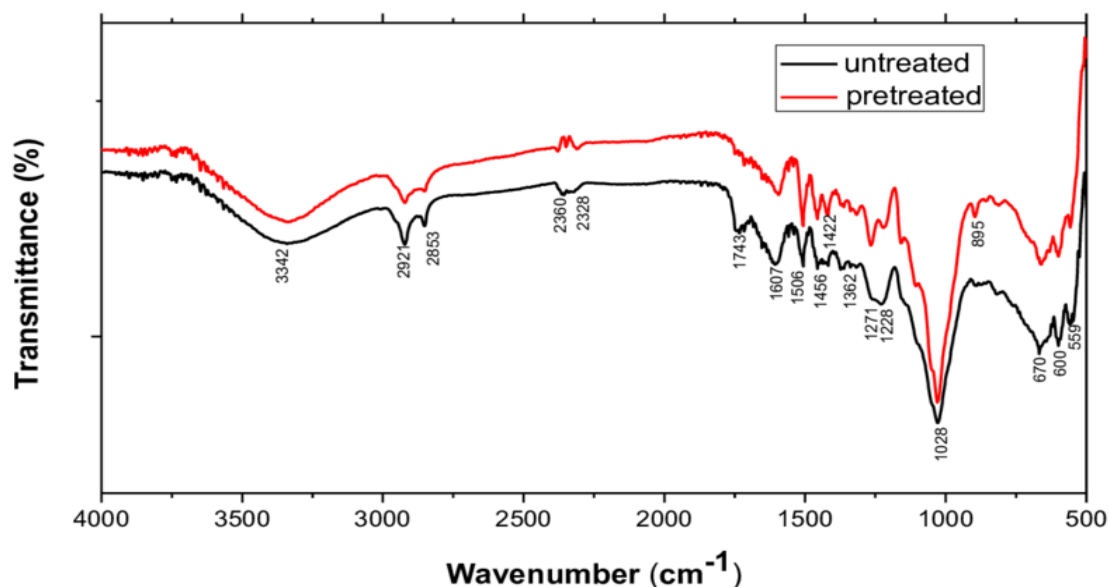


Fig. 9(A): Sterculie –foetede Raw & activated carbon –FTIR Spectra.

carbon) as CH₂ symmetric stretching 1641 cm⁻¹ as adsorbed OH water, 926 cm⁻¹ as β -glucosidic linkage, 1249 cm⁻¹ (Raw-carbon) as C–O stretch C–C stretch, 1040–1154 cm⁻¹ as antisymmetric stretching modes of the phosphate group, 1047 cm⁻¹ and 1249 cm⁻¹ as C–O stretching of phenolic compounds (lignin), additional peak at 1610 cm⁻¹ as stretching vibration of –C– C in [60] aromatic groups (Teli and Pandit, 2018b).

Fourier transform spectra of the Sterculia-foetida fiber fruit shell composite.		
Absorption frequency (cm^{-1})		
Wave number (cm^{-1})	Raw-carbon	Activated carbon
Symmetrical stretching O-H	3390 cm^{-1}	3400 cm^{-1}
O-H Stretching vibration Unsymmetrical	$3400\text{---}3300 \text{ cm}^{-1}$	$3529\text{---}3600 \text{ cm}^{-1}$
C-H stretching	2930 cm^{-1}	2256 cm^{-1}
CH ₂ symmetric stretching	1641 cm^{-1}	1752 cm^{-1}
C-O stretching	896 cm^{-1}	1020 cm^{-1}
C-C stretching	$1040\text{---}1090 \text{ cm}^{-1}$	$1125\text{---}1235 \text{ cm}^{-1}$
Antisymmetric stretching mode of phosphorus	1047 cm^{-1}	1154 cm^{-1}
C-O stretching	1249 cm^{-1}	1357 cm^{-1}
C = C Stretching vibration	1604 cm^{-1}	1781 cm^{-1}
C = C in aromatic groups	1610 cm^{-1}	1687 cm^{-1}

Table-6: Fourier transform spectra of the Sterculia-foetida fiber fruit shell composite.

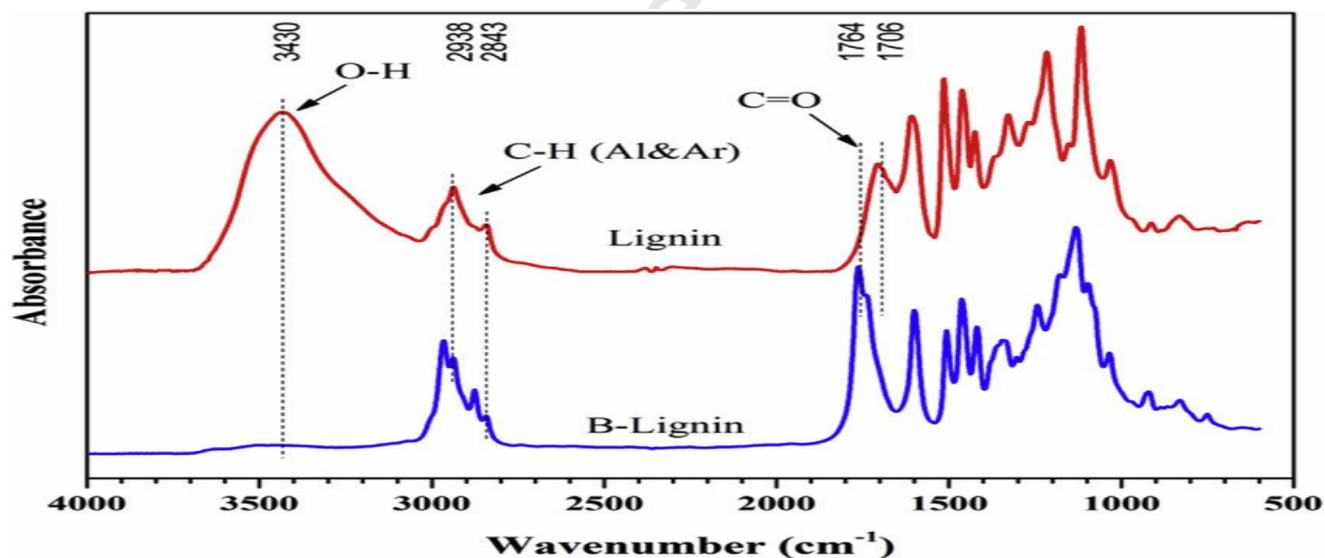


Fig. 9(B): FTIR Spectral Analysis of Lignin and B-Lignin Derived from *Sterculia foetida*

Observed Bands and Functional Groups

Wavenumber (cm^{-1})	Assignment	Functional Group	Structural Meaning
3390	O-H symmetric stretch	Hydroxyl (-OH)	Cellulose & hemicellulose hydrogen bonding
3400-3300	O-H asymmetric stretch	Broad hydroxyl band	Intermolecular H-bonding

Wavenumber (cm ⁻¹)	Assignment	Functional Group	Structural Meaning
2930	C–H stretching	Aliphatic –CH ₂ –/CH ₃	Polysaccharide backbone
1641	CH ₂ symmetric stretch / H–O–H bending	Bound moisture / cellulose	Indicates absorbed water
1604	C=C stretching	Aromatic	Lignin skeletal vibration
1610	Aromatic C=C	Lignin	Phenyl ring structure
1249	C–O stretching	Lignin / hemicellulose	Ether & phenolic groups
1040–1090	C–C stretching	Cellulose	Glycosidic linkage backbone
1047	P–O antisymmetric stretch	Phosphorus-containing group	Possible chemical activation or modification
896	C–O stretching	β-glycosidic linkage	Amorphous cellulose

Table-7: Observed bands and functional Groups of FTIR- *Sterculia-foetida* fiber fruit shell composite

4.5 Surface Area Analysis (BET) and Average particle diameter

Activated carbon with higher surface area (2.594×10^7 cm²/g) and total pore volume (1.67cm³g⁻¹) were extracted at a higher temperature of 600 °C. The total pore volume of *Sterculia foetida* shell-derived activated carbon under the influence of H₃PO₄ activation generally falls within the range of 1.2–1.8 cm³ g⁻¹, depending on the activation temperature, impregnation ratio, and carbonization conditions. In many experimental studies involving phosphoric acid activation of lignocellulosic biomass, the activated carbon obtained at higher temperatures (around 700–800 °C) shows a highly developed porous structure, resulting in a total pore volume of approximately 1.7–1.8 cm³ g⁻¹. The presence of H₃PO₄ promotes dehydration and cross-linking reactions during carbonization, which prevents structural collapse and facilitates the formation of micropores and mesopores within the carbon matrix. As a result, the activated carbon derived from *Sterculia foetida* shells exhibits large pore volume along with high surface area. The micropore volume (1.96cm³/g) gradually reduce with increased pyrolysis temperature, The micropore volume of *Sterculia foetida* shell-derived activated carbon generally decreases gradually with increasing pyrolysis temperature due to the widening and merging of micropores into mesopores and macropores. A typical trend observed during phosphoric acid (H₃PO₄) activation is shown below. which conformed the evolution of more micropores in the activated

carbon samples. A typical trend observed during phosphoric acid (H_3PO_4) activation is shown below

Pyrolysis Temperature ($^{\circ}C$)	Micropore Volume ($cm^3 g^{-1}$)
400 $^{\circ}C$	1.96
500 $^{\circ}C$	1.82
600 $^{\circ}C$	1.67
700 $^{\circ}C$	1.51
800 $^{\circ}C$	1.36

The BET surface area is one of the parameters that calculate the absorption capacity of the activated carbon. Higher surface area implies more accessibility, of surface for adsorption hence better adsorption capacity. The BET surface area and pore volume of both *sterculie-foetide* shell based raw, carbon and activated carbon particles were determined and shown in (Table 8).

When the pyrolysis temperature was 400 $^{\circ}C$, pyrolysis reaction had just commenced, thereby producing very small BET surface area and total volume. This phenomenon was due to the inadequate of heat energy to drive away any substantial amounts of volatiles. As the carbonization temperature [61] increased from 600 $^{\circ}C$ -800 $^{\circ}C$, H_3PO_4 increasingly greater volatile matters were released progressively during pyrolysis thereby resulting in the development of some new porosity, and hence BET surface area of the material and total volume (V_{tot}) of the porous increased, while the average diameter of the particle decreased. According to the pyrolysis results, the hemicellulose, cellulose and lignin in *Sterculie-foetide* fiber shell would take place dehydrating, linkage breaking off reactions, the structural ordering process of the residual carbon and finally happened polymerization [62], reaction during the carbonization process. With increasing carbonization temperature, polymerization reaction would be deepened, the diameter of sample would be lowered gradually and the micro porous sample would be developed, giving rise to increases in the BET surface area and total volume of micro porosity of carbon black. For example, the BET surface area of the carbon black obtained from *sterculie-*

.ACs	S_{BET} (m^2/g)	S_{μ} (m^2/g)	S_m (m^2/g)	V_T (cm^3/g)	V_{μ} (cm^3/g)	V_m (cm^3/g)	V_{μ}/T (%)	S_{μ}/S_{BET} (%)	D_p (nm)
H ₃ PO ₄ impregnation ratio: 3:2 (wt/wt) Activation temperature ($^{\circ}C$)									
400	2458	1931	587	1.59	1.45	0.07	97.75	77.98	2.48
500	2678	2124	4547	1.67	1.57	0.55	83.54	73.54	2.58

600	2594	1977	4796	1.79	1.96	0.87	86.52	72.51	2.79
700	2771	2552	499	1.52	1.65	0.54	84.37	71.47	2.58
800	2745	2445	495	1.68	1.84	0.69	83.75.	71.57	2.67
Activation temperature: 800 °C Impregnation ratio (wt/wt)									
1.1	2457	1948	579	1.77	1.75	0.52	77.28	87.53	2.38
1.2	2672	2445	485	1.69	1.55	0.47	76.52	79.52	2.58
2.1	2596	2097	479	1.87	1.77	0.59	74.59	76.51	2.69
3.2	2848	2455	474	1.67	1.85	0.47	73.52	75.52	2.48

S_{BET} : BET surface area, S_{μ} micropore surface area, S_m : mesopore surface area, V_T : total pore volume, V_{μ} : micropore volume, V_m : mesopore volume, $V_{\mu} \% = (V_{\mu} / V_T) \times 100$, $S_{\mu} \% = (S_m / S_{BET}) \times 100$, D_p : average diameter.

Table -8: BET surface area of Sterculie –foetide activated carbon composite.

foetide shell at 800°C was 2745 m²/g, presenting a rudimentary pore structure. Thus, higher temperature carbon black offers higher potential to produce activated carbon of greater adsorption. The prepared summary of BET surface area, total pore volume, micropore volume of Sterculie-foetide activated carbon composite capacity from sterculie-foetide shell. On the other hand, it was observed that, after chemical activation of raw sterculie-foetide fiber shell particles The BET surface area and total volume drastically increases with decreasing of average diameter as compared to the surface area of carbon black particles at various carbonization temperatures [63,64] and finally enters to nano range. It indicates that more previously inaccessible pore was opened and new pores were created with the chemical reaction between raw particles and hydrating agent in procession during the activation process. As a result, the BET surface area, total volume and average diameter of activated carbon prepared from raw sterculie-foetide fiber shell particles were 2745m²/g, 1.68cm³/g and 2.67nm at H₃PO₄ impregnation ratio: 3:2 (wt/wt) Activation temperature (800 °C).

5.1: Challenges in Implementation of Industrial-Scale Fiber Extraction of *Sterculia foetida*

The **industrial-scale extraction of fibers from *Sterculia foetida*** faces several technical, economic, and logistical challenges that limit its widespread commercialization. One of the major challenges is the **lack of standardized extraction techniques**, as most current studies are conducted at laboratory scale using manual or semi-mechanized retting and mechanical separation processes. Scaling these methods to industrial levels

requires specialized machinery capable of efficiently separating fibers without damaging their structure or reducing their mechanical properties. Another important issue is the **variability in raw material quality**, since the fiber yield and composition of *Sterculia foetida* depend on factors such as plant age, geographic location, climate conditions, and harvesting season. This variability can affect the consistency of fiber properties, which is critical for industrial applications such as composite reinforcement or carbon material production. Additionally, **efficient retting processes** (water, chemical, or enzymatic) remain a challenge because traditional retting methods are time-consuming and may produce unpleasant odors and environmental pollution due to microbial degradation.

From an economic perspective, the **high initial investment in processing infrastructure and fiber extraction equipment** presents a barrier for industries considering large-scale adoption. Transportation and storage of bulky biomass materials also increase operational costs. Moreover, there is **limited awareness and supply chain development** for *Sterculia foetida* biomass compared with established natural fibers such as jute, sisal, or coir, which restricts market availability and commercial interest. Another challenge is the **need for effective fiber treatment and purification processes**, including alkali treatment, bleaching, and drying, to enhance fiber quality and compatibility with polymer matrices or carbonization processes. Environmental considerations also play a significant role, as industrial extraction must ensure **sustainable biomass harvesting and eco-friendly processing methods** to avoid deforestation or ecological imbalance. Therefore, overcoming these challenges requires the development of **advanced mechanized extraction technologies, optimized pretreatment processes, sustainable harvesting practices, and integrated biomass utilization strategies** to make *Sterculia foetida* fiber extraction economically viable and environmentally sustainable at an industrial scale

Sterculia -foetida fiber extraction from laboratory to industrial level introduces multiple technical, economic, environmental, and characterization challenges; Seasonal availability Variation in bark thickness & fiber content, Moisture content fluctuations, Supply chain inconsistency Technical Issues: Large-scale water retting requires: Huge water consumption Long processing time (7–14 days Environmental Concerns: High COD/BOD wastewater, Phosphate contamination, Solid sludge disposal drying & Storage Problems Industrial Barriers :High energy

demand for drying, Moisture reabsorption in humid climates, Fungal growth during storage
Structural Characterization (XRD, FTIR, SEM) Problems: Batch-to-batch structural variability
Inconsistent crystallinity index Variation in cellulose/lignin ratio Surface chemistry inconsistency.
Mechanical Property Testing Tensile strength variation, Diameter irregularity, Non-uniform fiber
orientation, Lack of standardized testing protocols for *Sterculia foetida* Surface & Porosity
Analysis (If used for Activated Carbon) BET surface area variability, Pore size distribution
inconsistency, Residual mineral content variation Economic & Commercial Challenges.

5.2 : Specific Applications

Sterculia foetida fiber reinforced composites and activated carbon derived from its biomass have several specific engineering and environmental applications due to their lightweight structure, good mechanical strength, and high surface area. In the **automotive industry**, *Sterculia foetida* fiber-reinforced polymer composites can be used for manufacturing interior **door panels, dashboard components, seat back panels, and trunk liners**, where lightweight and eco-friendly materials are required to improve fuel efficiency. In the construction sector, these fibers can be incorporated into fiber-reinforced cement boards, partition panels, **ceiling boards, and insulation materials**, providing improved crack resistance and reduced structural weight. Additionally, when converted into activated carbon and incorporated into composite matrices, the material can be used in water purification systems such as adsorption filters for removing **dyes, heavy metals, and organic pollutants** from industrial wastewater,

Particularly in textile and chemical industries. The high porosity of activated carbon derived from *Sterculia foetida* also makes it suitable for **electrode materials in supercapacitors and energy storage devices**, where large surface area and electrical conductivity are important. Furthermore, composite matrices containing *Sterculia foetida* carbon materials can be applied in air purification filters, gas adsorption systems, and protective filtration units for removing volatile organic compounds (VOCs) and toxic gases. In **environmental remediation**, these materials can be utilized for oil spill adsorption and soil pollutant removal, owing to their porous carbon structure and adsorption capacity. Therefore, the integration of *Sterculia foetida* fiber and activated carbon in composite matrices offers promising industrial, environmental, and energy-related applications with sustainable and renewable material advantages

Application–Characterization Mapping

Application	Key Characterization
Automotive composite	Tensile, SEM, XRD
Geotextile	Moisture, TGA
Activated carbon	BET, XRD, FTIR
Biopolymer reinforcement	FTIR, crystallinity
Insulation panels	Thermal conductivity
Paper industry	Cellulose %, fiber length

5.0 : Conclusion and future perspective

To develop a scalable extraction process for *Sterculia foetida* fiber: The study demonstrates that mechanical decortication combined with controlled chemical retting (alkali or mild acid treatment) can be adapted for industrial-scale processing. Process optimization reduced retting time and improved fiber separation efficiency. However, water consumption, effluent management, and raw material variability remain key scale-up constraints. Implementation of closed-loop water recycling and standardized pretreatment protocols is essential for commercial viability.

To evaluate the structural properties using XRD, FTIR, and SEM: XRD analysis confirmed the semi-crystalline cellulose structure, with characteristic diffraction peaks corresponding to cellulose. FTIR spectra indicated the presence of hydroxyl (–OH), carbonyl (C=O), and lignocellulosic functional groups, confirming the natural fiber composition. SEM micrographs revealed rough surface morphology favorable for matrix adhesion in composite applications. Industrial batches showed minor variation in crystallinity index, indicating the need for strict process control to ensure consistency.

To determine mechanical and thermal properties for industrial applicability:

Tensile strength and Young's modulus values suggest that *Sterculia foetida* fiber is suitable for medium-load composite reinforcement applications. Thermogravimetric analysis indicated thermal stability up to ~250–300 °C, making the fiber compatible with thermoset and selected thermoplastic matrices. Moisture absorption behavior highlights the importance of surface modification prior to composite manufacturing

To assess industrial feasibility and potential applications: Based on physicochemical and mechanical characterization, the extracted fiber shows strong potential for: Automotive interior composite panels Biodegradable packaging boards Geotextiles and erosion control mats Acoustic and thermal insulation materials Precursor material for activated carbon However, industrial implementation requires: Standardization of fiber dimensions Efficient effluent treatment systems Cost optimization compared to conventional fibers (jute/coir)

To analyze sustainability and environmental impact: The fiber extraction process aligns with sustainable material development goals, as it utilizes renewable biomass. Nevertheless, large-scale chemical retting may introduce environmental burdens unless eco-friendly treatment and wastewater recycling technologies are incorporated. Life cycle assessment is recommended before commercialization. The industrial-scale extraction and characterization of *Sterculia foetida* fiber demonstrate its viability as a sustainable lignocellulosic reinforcement material. Structural (XRD, FTIR), morphological (SEM), and mechanical analyses confirm its semi-crystalline cellulose framework, adequate tensile properties, and thermal stability suitable for composite and industrial applications. Although promising, successful commercialization depends on process standardization, environmental management, and economic competitiveness. With optimized industrial protocols, *Sterculia foetida* fiber can emerge as a valuable alternative natural fiber in green material engineering.

- ✚ The lower atomic ratio of H/C (0.09–0.05) and O/C (0.52–0.07) of carbon composite confirmed that they were highly carbonized and hydrophobic
- ✚ The FTIR analysis observed that the pyrolysis process significantly removes the polar and acidic functional groups from activated carbon with increasing pyrolysis temperature
- ✚ Activated carbon with higher surface area ($2.594 \times 10^7 \text{ cm}^2/\text{g}$) and total pore volume ($1.67 \text{ cm}^3/\text{g}^{-1}$), the micropore volume ($1.96 \text{ cm}^3/\text{g}$) were obtained at a higher temperature of $600 \text{ }^\circ\text{C}$ which show the evolution of more micropores in the activated carbon samples gradually decreased with increased pyrolysis temperature.
- ✚ From the characterization of activated carbon, it was finishing that the pyrolysis temperature of $600 \text{ }^\circ\text{C}$ was the most effective pyrolysis temperature in terms of surface area, total pore volume and high mass fraction of carbon and fixed carbon, for both the

biomass materials. This study approved that biomass composition and pyrolysis temperature had a great effect on activated carbon yield, morphological and physicochemical characterization.

- ✚ The proximate and chemical characterization ratified that both the experimental result of chemical composition, it is noticed that raw sterculie –foetede fiber shell particles have higher cellulose and lignin content Thus it is likely to produce activated carbon with higher micro porosity. From proximate analysis result, it is finalized that the fixed carbon percentage of raw sterculie –foetede shell particles increases from 19.11% to 94.5% after activating with chemical activating agent at 800°C activated temperature
- ✚ XRD studies reveals that the main constituents of sterculie –foetede carbon based was mostly graphite and amorphous carbon. The surface functional groups of the sterculie –foetede fiber shell activated carbon were generally neutral (or slightly acidic), which would explain the dependence of the adsorptive capacity for both acidic and basic gases on the textural characteristics of the activated carbon. XRD characterization accepted the presence of higher inorganic compounds such as calcite, quartz, and silicates of Mg, Ca, and Mn in bamboo-derived activated carbon than pigeon pea stalk activated carbon at the same pyrolysis temperature
- ✚ TGA curve of raw, carbonized and activated carbon of both sterculie –foetede fiber shell particles shows that initial decrease in weight loss completed below 150°C is due to the moisture loss from the material at this temperature. Due to activation, in both cases the carbon content are increases hence the carbon has higher the material's opposition to heat flow acting like electrical resistance (thermal resistance).
- ✚ The carbonization temperatures had great effects on the pore developed by expanding of the carbon black extracted with increasing of carbonization temperatures, more volatiles were released and more micropores were obtained which increases the BET surface area of the carbon particles and total volume of the pore as well as reduce the radius of the carbon particles.
- ✚ Scanning electron microscope images gives a view about the pores present on the surface of raw carbon black & activated carbon composites of both sterculie –foetede shell from

it is inferred that, there was no pore visible on the surface of raw material, but there were clearly visible pores in case of activated carbon. In SEM analysis also, it is clearly shown the particle size of the filler and the average particle size of the raw sterculie –foeitede fiber shell are 2.5 microns and the activated carbon from sterculie –foeitede is 97 nano meters.

- Due to activation of the particulates the strength of the composite is increased and also lower the empty gaps within a material (Void content) in the composites. The results of flexural strength and tensile strength of (raw carbon black & activated carbon black) of sterculie –foeitede, it is found that observed the composite gives highest strength, modulus and hardness compared with other activated and non- activated particulates composite

Declaration of competing interest:

The authors declare that they have no known competing financial interests or personal relationships that could have appeared to influence the work reported in this paper.

CRedit authorship contribution statement:

Srinivasa Rao Pedada: Software, Resources, Methodology, Data curation. Srinivas Rao Golagani: Software, Resources, Methodology, Data curation. Manoj Kumar Regulagadda: Validation, Software, Resources, Ch V KameswaraRao, Formal analysis. Anitha Kumari Mosya: Writing – review & editing, R. S. S. Srikanth Vemuri, Visualization, Validation, Resources.

Data availability:

No data was used for the research described in the article.

References

- [1] Y.Wang, S. Xu , K.H. Bwar, B. Eisenbart, G. Lu, A. Belaadi, B. Fox, B.X.Cha Application of machine learning for composite moulding process *modelling Composites Communi cations*, 48 (2025) 101906 ,<https://doi.org/10.1016/j.coco.2024.101960>
- [2] Yuqi.Feng,Huali Hao,Haibao Lu,Cheuk Lun Chow Denvid Lau, Exploring the development and applications of sustainable natural fiber composites: A review from a nanoscale perspective, *Composites Part B: Engineering*,776 (2024)111369.

- [3] Pintu. Pandit, M.D.Teli, Kunal.Singha, Saptarshi. Maiti. Extraction and characterization of novel *Sterculia foetida* fruit shell fiber for composite applications, *Cleaner Engineering and Technology*,4 (2021) 109194.
- [4] Peng Huo, Shaochun Ma Lingfeng Li, Wenpeng. Liang,Jianlin Mo, Bosheng Zeng Hongliang Nong Zhengliang Ding Weiqing Li, Influence of tensile properties and fiber fraction on the mechanical properties of the sugarcane top anti-tangling in the silage industry, *Industrial Crops and Products*,208 (2024)117898 .
- [5] KaushalKishor,MukeshKumarSingh,Supriyo.Chakraborty,Extractionand characterization of cattail fiber and lignin recovery from retting bath, *Bioresource Technology Reports*, 25 (2024) 101753.
- [6] Samuel. Garriba Samuel. H. Garriba, Siddhi. Jailani Extraction and characterization of natural cellulosic fiber from *Mariscus ligularis* plant as potential reinforcement in composites, *International Journal of Biological Macromolecules*, 253 (2023) 127609.
- [7] Pintu.Pandit M.D.Teli, Kunal. Singha, Saptarshi. Maiti. Subhankar, Maity, Extracting and characterizing novel cellulose fibers from *Chamaerops humilis* rachis for textiles' sustainable and cleaner production as reinforcement for potential applications, *Cleaner Engineering and Technology*, 14 (2021) 100194.
- [8] Mouad.Kir,Mohamed.Boudiaf,AhmedBelaadi,Messaouda,Boumaaza.Mostefa,BourchakDjamel Ghernaout, Extracting and characterizing of a new vegetable lignocellulosic fiber produced from *C. humilis* palm trunk for renewable and sustainable applications, *International Journal of Biological Macromolecules*,284 (2024) 136495.
- [9] A..Arul, Marcel. Moshi ,D. Ravindran,S.R.Sundara Bharathi, S.Indran,S.S. Saravanakumar Yucheng. Liu, Characterization of a new cellulosic natural fiber extracted from the root of *Ficus religiosa* tree nternational, *Journal of Biological Macromolecules* 276 (2024) 134029.
- [10] Oussama.Ferfari,Ahmed.Belaadi,Azzeddine. Bedjaoui, Amar. Al-Khawlani, Mohammad. K.A. Khan, Characterization of a new cellulose fiber extracted from *Syagrus Romanzoffiana* rachis as a potential reinforcement in bio composites materials, *Materials Today Communications* 36 (2023) 106576.
- [11] Abdelwaheb Hadou, Ahmed. Belaadi, Hassan. Alshahrani, Mohammad. K.A. Khan, Extraction and characterization of novel cellulose fibers from *Dracaena draco* plant Materials, *Science Communications*, 313 (2024) 128790.
- [12] A.C.Jadhav.Pandit. P, Gayatri,T.N, Chavan. P.P, N.C. Jadhav. Production of Green composites from various sustainable raw materials. *Green Composites*. Springer (2019)1-24, https://doi.org/10.1007/978-981-13-1969-3_1.
- [13] D.Gon, K Das.. P.Paul, S, Maity, Jute composites as wood substitute. *Int. J. Textil. Sci.* 1 (6)(2013.) 84–93. <https://doi.org/10.5923/j.textile.20120106.05>.
- [14] S.Maity. D.P Gon, P.A Paul, Review of flax nonwovens: manufacturing, propertiesand applications.*J.Nat.Fibers*,11(4)(2014.)365–390. <https://doi.org/10.1080/15440478>
- [15] S, Maity, Jute need launched nonwovens: manufacturing, properties, and applications.*J. Nat. Fibers*, (2016). <https://doi.org/10.1080/15440478.2015.1029200..>

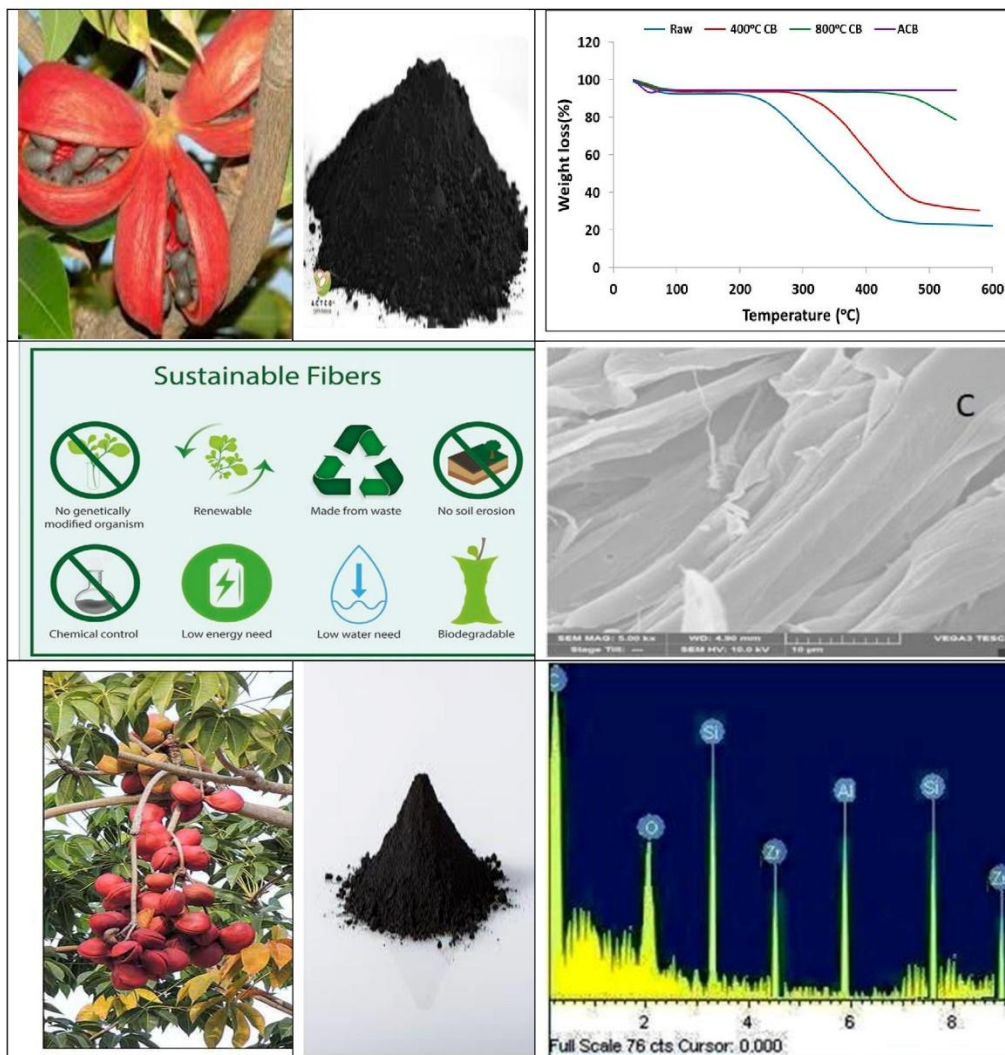
- [16] R Liu, Xiao. H, S.D., J. .Pang, H.Yang, Application of Sterculia foetida petiole wastes in lightweight pervious concrete *J. Clean. Prod.*246(2020) 118972 <https://doi.org/10.1016/j.jclepro.2019.118972>.
- [17] M.D. Teli, A.C. Jadhav, Extraction and characterization of novel lignocellulosic fiber *J. Bio nanoscience* 10 (5) (2016) 418–423. <https://doi.org/10.1166/jbns.2016.1392>.
- [18] M.D.. Teli, P. Pandit, A novel natural source sterculia foetida fruit shell waste as colorant and ultraviolet protection for linen. *J. Nat. Fibers* 15 (3), (2018a) 337–343. <https://doi.org/10.1080/15440478.2017.1328327>
- [19] A.Ray, K Singha,, P .Pandit, S.Maity Advanced ultraviolet protective agents for textiles and clothing. In: *Advances in Functional and Protective Textiles*. Wood head Publishing, (2020).243–260. <https://doi.org/10.1016/b978-0-12-820257-9.00011-4>
- [20] M.D Teli, P.Pandit, Application of Sterculia- foetida fruit shell waste biomolecules on silk for aesthetic and wellness properties. *Fibers Polym.* 19 (2018b) 41–54. <https://doi.org/10.1007/s12221-018-7315-4>.
- [21] P.Pandit K. Singha, S Maity, Green chemistry in textile and fashion. In: *Chemical Management in Textiles and Fashion*. Woodhead Publishing, (2021)177-203. <https://doi.org/10203>. <https://doi.org/10.1016/b978-0-12-820494-8.00009-5>
- [22] Bajpai. Pramendra Kumar, Inderdeep Singh, Jitendra Madaan, Tribological behavior of natural fiber reinforced PLA composites, *Wear*,299 (2013,) 829-840.
- [23] A Ticoalu, T.Aravinthan, F. Cardona, A review of current development in natural fiber composites for structural and infrastructure applications, *Proceedings of the Southern Region Engineering Conference (SREC '10)*, (2010), Toowoomba, Australia, 113–117, 2-s2.0-84877640742.
- [24] Rajesh, Y., Gautam, N. B., Shah, J., Thandlam, A. K., Gole, S., Nirgude, P., & Dabhade, G. B. (2024). Evaluation of activated biochar from sustainable *Sterculia foetida* shells for the removal of Acid Blue 158 dye. *Journal of Environmental Nanotechnology*, 13(2), 248–255. <https://doi.org/10.13074/jent.2024.06.242607>
- [25] Zhang, Y., Li, X., Wang, J., Chen, H., Liu, Q., & Zhao, Y. (2023). Synthesis and applications of biomass-derived porous carbon materials in energy utilization and environmental remediation. *Chemosphere*, 339, 139635. <https://doi.org/10.1016/j.chemosphere.2023.139635>
- [26] L. Wang, T. Wang, R. Hao, and Y. Wang, “Synthesis and applications of biomass-derived porous carbon materials in energy utilization and environmental remediation,” *Chemosphere*, (2023).339,139635, <https://doi.org/10.1016/j.chemosphere.2023.139635>
- [27] Y. Rajesh, N. B. Gautam, J. Shah, A. K. Thandlam, S. Gole, P. Nirgude, and G. B. Dabhade, “Evaluation of activated biochar from sustainable *Sterculia foetida* shells for the removal of Acid Blue 158 dye,” *Journal of Environmental Nanotechnology*,.(2024) 13,248–255,. <https://doi.org/10.13074/jent.2024.06.242607>
- [28] P.Pandit,S.Maiti,T.N.Gayatri, A. Mallick ,Applications of textile materials using emerging sources and technology: a new perspective. In: *Green and Sustainable Advanced Materials: Applications*,2(2018b) 49–83. <https://doi.org/10.1002/9781119528463.ch3>

- [29] N.Wang, B. Xu, X.Wang, J. Lang, & H. Zhang, Chemical and structural elucidation of lignin and cellulose isolated using des from bagasse based on alkaline and hydrothermal pretreatment. *Polymers (Basel)*,14 (2022).
- [30] K. X. Zhu, S. Huang, W. Peng, H. F Qian. H. M. Zhou, Effect of ultrafine grinding on hydration and antioxidant properties of wheat bran dietary fiber. *Food Res. Int.* 43 (2010) 943–948.
- [31] M.Zhang, et al. The structure and properties of lignin isolated from various lignocellulosicbiomassbydifferenttreatmentprocesses.*Int.J.BiolMacromol.*243(2023) 125219 .
- [32] H.Zhou et al., Synthesis of honeycomb lignin-based biochar and its high-efficiency adsorption of norfloxacin. *Bioresour. Technol.* 369 (2023) 128402.
- [33] T. R.Nunn, J. B. Howard, J. P.Longwell, W. A. Peters, Product compositions and kinetics in the rapid pyrolysis of sweet gum hard wood. *Industrial & Engineering Chemistry Process Design and Development*, 24(3) (1985) 836-844.
- [34] A. Zeriuoh, & L. Belkbir,Thermal decomposition of a Moroccan wood under a nitrogen atmosphere,*Thermochimica acta*, 258 (1995)243-248.
- [35] F.Wu, et al. Industrial alkali lignin-derived biochar as highly efficient and low-cost adsorption material for Pb(II) from aquatic environment. *Bioresour. Technol.* 322 (2021) 124539.
- [36] Boopathi, G., Ragavan, R., Jaimohan, S.M., Sagadevan, S., Kim, I., Pandurangan, A., & Sivaprakash, P. Mesoporous graphitic carbon electrodes derived from boat-fruited shells of *Sterculia foetida* for symmetric supercapacitors for energy storage applications. *Chemosphere*, (2024), 348, DOI: 10.1016/j.chemosphere.2023.140650
- [37] Sivaraman, S., & Selvasembian, R. Pyrolysis behavior of *Sterculia guttata* shell biomass: kinetics, thermodynamics and industrial biochar production, *RSC Advances*,(2026).DOI: 10.1039/D5RA09614F
- [38] Selva, S.J., Michael, M.S. Feasibility of Hydrothermal Activation for Conversion of Biomass of *Sterculia Foetida* into Hard Carbon Anode for Sodium-Ion Battery. *Bioenerg. Res.* (2026).19, 16 <https://doi.org/10.1007/s12155-025-10953-6>.
- [39] Souza, et al. Valorization of andiroba (*Carapa guianensis* Aubl.) residues through optimization of alkaline pretreatment to obtain fermentable sugars. *Bioresources* 15 (2020) 894–909.
- [40] G. Gayathri, & K. B Uppuluri, The comprehensive characterization of *Prosopis juliflora* pods as a potential bioenergy feedstock. *Sci. Rep.* 12 (2022) 1–13.
- [41] B. Xu, Wang, Wang, X., Lang, J. & Zhang, H. Experimental study on the separation of bagasse lignin and cellulose by using deep eutectic solvent based on alkaline pretreatment.*BiomassConvers.Biorefin.*(2022).<https://doi.org/10.1007/s13399-022-03110-y>
- [42] S, N. Dhara, N. S. Samanta, R Uppaluri,. & M. K Purkait, High-purity alkaline lignin extraction from *Saccharum ravannae* and optimization of lignin recovery through response surface methodology. *Int. J. Biol Macromol.* 234 (2023) 123594.
- [43] J Sarki., S. B. Hassan, V. S. Aigbodion, & J. E. Oghenevweta, Potential of using coconut shell particle fillers in eco-composite materials. *Journal of alloys and compounds*, 509(5) (2011) 2381-2385.
- [44] T.Hahn Dordrecht, Space-group symmetry: *International Tables for Crystallography*. Volume A. 5th edition. Kluwer Academic Publishing; 2002.

- [45] W. Ruland , X-ray determination of crystallinity and diffuse disorder scattering. *Acta Cryst* 14 (1961)1180-1185.
- [46] C.J.Garvey,IH.Parker, GP.Simon,On the interpretation of X-ray diffraction powder patterns in terms of the nanostructure of cellulose I fibres. *Macromol Chem Phys*, 206(2005)1568-1575.
- [47] J..He, S. Cui., S.Y. Wang, Preparation and crystalline analysis of high-grade bamboo dissolving pulp for cellulose acetate. *J Appl Polym Sci* 107 (2008) 1029-1038.
- [48] S. Park, J. O. Baker, M. E. Himmel, P. A. Parilla, & D. K. Johnson, Research cellulose crystallinity index: measurement techniques and their impact on interpreting cellulase performance. *Biotechnol Biofuels*, 3(10) (2010).
- [49] Sridharan, V., Pulidindi, I.N., Vaithyanathan, P., Kanthadai, V.T., & Balasubramanian, V. Steam activated carbon material from the fruit shells of *Sterculia foetida* for energy and environmental applications. *Journal of Water Pollution & Purification Research* (2024).11,23-33
- [50] Rajamani, R., Kumar, B.V., & Sujith, A. *Sterculia foetida* fruit shell based activated carbon for the effective removal of industrial effluents. *Journal of the Indian Chemical Society* (2021). DOI: <https://doi.org/10.1016/j.jics.2021.100196>
- [51] F. G .Emmerich, J. C. De Sousa, I. L Torriani,. C. A. Luengo,. Applications of a granular model and percolation theory to the electrical resistivity of heat-treated endocarp of babassu nut. *Carbon*, 25(3) (1987) 417-424.
- [52] S. Sohni, et al. Physicochemical characterization of Malaysian crop and agro-industrial biomass residues as renewable energy resources. *Ind. Crops Prod.* 111(2018) 642–650.
- [53] H.Klug, L Alexander. X-ray Diffraction Procedures for Polycrystalline and Amorphous Materials. 2nd edition. New York: John Wiley & Sons; 1974.
- [54] R Jenkins, R. Snyder, *Introduction to x-ray powder diffractometry. In Chemical Analysis* Volume 138. New York: John Wiley & Sons; 1996.
- [55] A. C Lua, & T. Yang, Effect of activation temperature on the textural and chemical properties of potassium hydroxide activated carbon prepared from pistachio-nut shell. *Journal of colloid and interface science*, 274(2) (2004) 594-601.
- [56] M..Kumar, & R. C. Gupta, Influence of carbonization conditions and wood species on carbon dioxide reactivity of resultant wood char powder. *Fuel processing technology*, 38(3) (1994) 223-233.
- [57] W.Tongpoothorn, M Sriuttha. P. Homchan, S.Chanthai, & C. Ruangviriyachai, Preparation of activated carbon derived from *Jatropha curcas* fruit shell by simple thermo-chemical activation and characterization of their physico-chemical properties. *Chemical Engineering Research and Design*, 89(3) (2011) 335-340.
- [58] .Zhao, J, L. Yang, F. Li, R. Yu, & C. Jin, Structural evolution in the graphitization process of activated carbon by high-pressure sintering. *Carbon*, 47(3) (2009) 744-751.
- [59] Pedada. Srinivasa Rao , Golagani. Srinivas Rao , Regulagadda. Manoj Kumar, Mosya Aitha Kumari, Study and characterization of *Sterculia foetida* (Java olive) activated carbon black Filled composite materials, *Results in Chemistry*,13(2025)102003.

- [60] Teli, M.D. P. Pandit. Application of Sterculia foetida fruit shell waste biomolecules on silk for aesthetic and wellness properties. *Fibers Polym.* 19(2018b)4154 <https://doi.org/10.1007/s12221-018-7315-4>.
- [61] S.Yorgun, Yildiz, Preparation and characterization of activated carbons from Paulownia wood by chemical activation with H_3PO_4 . *J Taiwan Inst Chem E*, 53 (2015) 122–31.
- [62] YPrahaskartika, N.Indraswati, S.Ismadji, Activated carbon from jackfruit peel waste by H_3PO_4 chemical activation pore structure and surface chemistry characterization *Chem Eng J* 140 (2008) 32–42.
- [63] NV.Sych, SI.Trofymenko, OI.Poddubnaya, MM.Tsyba, VI.Sapsay, DO.Klymchuk, AM.Puziy, Porous structure and surface chemistry of phosphoric acid activated carbon from corncob, *Appl Surf Sci*, 261 (2012) 75–82.
- [64] A. Kumar et al, High surface area microporous activated carbons prepared from Fox nut (*Euryale ferox*) shell by zinc chloride activation. *Applied Surface Science*, 2015, 356, 753-761.

Graphical abstract



HIGHLIGHTS

- ✚ Activated carbon with higher surface area ($2594\text{m}^2/\text{g}$) and total pore volume ($1.79\text{ cm}^3\text{g}^{-1}$), the micropore volume ($1.96\text{cm}^3/\text{g}$) were obtained at a higher temperature of $600\text{ }^\circ\text{C}$
- ✚ The FTIR analysis showed that the pyrolysis process significantly removes the polar and acidic functional groups from activated carbon with increasing pyrolysis temperature.
- ✚ Thermo gravimetric curves of raw carbon and activated carbon of both sterculie –foeitede fiber shell particles shows that initial decrease in weight loss completed below 150°C is due to the moisture loss from the material
- ✚ It is observed that Sterculie –foeitede, fiber shell particulates composite gives highest strength, modulus and hardness compared with other activated and non- activated particulates composite
- ✚ In SEM analysis it is clearly shown the particle size of the fiber filler and the average particle size of the raw sterculie –foeitede fiber shell are 2.5 microns and the activated carbon is 97 nano meters